Integrated Micro-Scale Concentrating Photovoltaics: A Scalable Path Toward High-Efficiency, Low-Cost Solar Power

Norman Jost,* Tian Gu, Juejun Hu, César Domínguez, and Ignacio Antón

The global energy market is seeing increases in the electricity demand of a couple of percentage points annually. The photovoltaic (PV) industry is also growing rapidly every year. One of the PV technologies is concentrator photovoltaics (CPV). CPV uses high-efficiency multijunction solar cells and optics to concentrate sunlight, thereby significantly reducing the amount of semiconductor material needed. Yet, due to the high upfont manufacturing cost of CPV, it currently does not offer a competitive price against silicon PV. With this a new branch is introduced to the industry, micro-CPV, which can be broadly explained as the miniaturization of the solar cells and optical components. The motivation for micro-CPV is lowering the cost by decreasing the material volume and enabling new system architectures and high-throughput manufacturing methods, while still maintaining high electrical efficiencies, taking advantage of a lower thermal load, shorter optical paths, lower resistive losses, and lower material volumes. Herein, a comprehensive review of the technological advances is presented, key synergies between micro-CPV and other industries sharing similar challenges are identified, exemplified by micro-light emitting diodes display manufacturing. New assembly process development in these industries will facilitate commercial adoption of micro-CPV with continued miniaturization while driving down the cost.

N. Jost, C. Domínguez, I. Antón
Instituto de Energía Solar
Universidad Politécnica de Madrid
28040 Madrid, Spain
E-mail: norman.jost@upm.es

T. Gu, J. Hu
Department of Materials Science & Engineering
Massachusetts Institute of Technology
Cambridge, MA 02139, USA

C. Domínguez
ETS Ingeniería y Diseño Industrial
Universidad Politécnica de Madrid
28012 Madrid, Spain

The ORCID identification number(s) for the author(s) of this article can be found under https://doi.org/10.1002/solr.202300363.

1. Introduction: The Promise of Micro-CPV Technology

In recent years, photovoltaic (PV) solar energy has undergone dramatic production growth and price reduction, leveraging the economy of scale of silicon-based PVs that dominate the market. As the efficiency of silicon cells reaches the practical limit, PV technologies with better performance become critical for a sustainable price learning curve of solar power.[1,2] Nevertheless, as silicon PV has become a commodity nowadays, any emerging technology inevitably faces the scaling dilemma between cost and volume at initial stages. On the other hand, the quest for high-power density PV has long been called out in fast-rising markets, such as low-cost space solar, vehicle integrated PV, mobile solar charging systems, robotics, and other area-constrained applications. Thereby high-efficiency and low-cost PV technologies beyond Si are essential to enable further market penetration of solar power and potentially a new price learning curve.

Concentrator PV (CPV) that use refractive and/or reflective optical components to focus sunlight onto solar cells had been conceptualized and developed since the birth of solar cells with the promise of high performance at low costs. By employing high-efficiency multijunction cells and optical concentrators, CPV technologies considerably reduce the usage of semiconductor materials which in principle decreases energy production cost.[3–9] Meanwhile, the high-power output provided by CPV also potentially allows reduction of area-related costs at the system level, such as balance-of-system and land usage. Meanwhile, CPV performance has been improving steadily in recent years, with cell and module conversion efficiencies reaching over 47% and 43.4%, respectively.[10,11]

While to the first order, the optical concentrators could dramatically reduce the usage of costly semiconductor materials (e.g., 200X–1000X geometric concentration ratios), the incorporation of discrete macro-scale concentrators brings in trade-offs among materials costs, module fabrication costs (e.g., complex optics and module manufacturing) at the module level and installation and operation costs (e.g., bulky panel form factor and specialized high-precision sun trackers) at the system level.[8,12]

Improvement on the concentration ratio and thus reduction of the multijunction cell area rely on increased complexity of the optical concentrator system, which inevitably increases module fabrication costs. Furthermore, conventional concentrator optics poses stringent requirements on tracker accuracy, mandating dedicated CPV trackers incompatible with low-cost trackers designed for silicon PV. Moreover, due to the relatively small acceptance angles, conventional CPV architectures cannot capture the diffuse component of sunlight (i.e., light scattered by atmospheric aerosols and clouds), which constitutes a considerable portion of the total incident power. According to standard solar radiation data across the USA, diffuse radiation contributes to approximately 2–2.5 kWh m^{-2}-day for all the locations studied, representing 20–40% of the global radiation depending on the geographic location.[13,14] The inability of CPV to capture diffuse light further limits its deployment and market penetration.

The cost and performance challenges associated with CPV are imposed by the thermodynamic limit of optical concentrators. A fundamental trade-off exists between geometrical concentration ratio (X) and acceptance angle (θ_{in}, defined as the light incident angle at which the optical collection efficiency drops to 90% of that at normal incidence), which is also known as the conservation of étendue.[15,16] To evaluate different CPV architectures and systems, a key figure of merit (FOM) is defined as the concentration-acceptance product (CAP).[17]

$$CAP = \sqrt{X}\sin\theta_{in} \qquad (1)$$

In theory, for a given optical concentrator architecture, CAP is nearly an invariant for different designs with different concentration ratios. This FOM, however, can be improved by using advanced optical architectures, e.g., by increasing the number of optical elements or using non-imaging optics tailored for light collection.[18–20] Such approaches, on the other hand, will increase the module complexity and fabrication costs. Therefore, Equation (1) not only reveals the trade-off between concentration ratio and acceptance angles but also the balance among materials, module, and system-level costs. Traditional CPV systems can achieve CAP values close to or below 0.7 and are typically designed for high concentrations aiming to reduce cell costs.[9] As a result, this is usually accompanied by complex module designs and tight tolerances to assembly and operation misalignments.[3] For example, for CPV systems with 1000X concentration ratio or above, high-precision module assembly and high-accuracy trackers (<1°) are necessary. Such requirements result in high module fabrication and BOS costs that offset the performance and cost improvements at the cell level.

Conventional CPV technology was not able to fulfill the promise of simultaneously achieving high performance and cost reduction, trapped in a chicken- or-egg paradox. The lack of sufficient commercial deployment has prevented the benefit of cost reduction associated with the learning curve of the technology, whereas the lack of competitiveness compared to conventional PV prevented large-scale market development of the technology. In order to reach or even surpass the cost learning curve of silicon PV technology, the following key performance attributes are demanded to improve existing CPV technologies: 1) high efficiency multijunction solar cells, 2) high concentration, high-efficiency optical concentrator for reduced usage of semiconductor materials, and enhanced performance, 3) sufficient field-of-view accommodating pointing accuracies of low-cost trackers (1°–1.5° tracking accuracy), 4) compact and simple module designs that minimize assembly and installation costs, 5) low thermal loads and mechanical stress, 6) module fabrication and BOS compatible with current silicon PV infrastructures to leverage the economy of scale, 7) cost-effective diffuse light collection, and 8) cross-pollination with other industrial technologies conducive to a fast learning curve to accelerate the cost reduction and competitiveness.

In recent years, a new class of PV technologies, i.e., micro-CPV, have attracted significant R&D efforts.[14,21–32] The technologies have shown a strong potential to address the aforementioned cost issues at both module and system levels while fulfilling the high performance of multijunction cells. Micro-CPV technologies leverage modern micro-fabrication and assembly techniques to dramatically scale down the dimensions of solar cells (with sizes of 100's of microns up to 1 mm) and accordingly the optical systems (diameters in the range of a few millimeters to a few centimeters) in novel module architectures. Arrays of micro-cells and micro-optics are tightly integrated within an ultra-compact flat module similar to silicon PV using advanced cell fabrication and massive parallel assembly approaches compatible with large-scale manufacturing.

As detailed in later sections, potential module-level benefits of exploiting such dimension downscaling include improved cell-to-module power ratio, increased optical efficiency, enhanced heat dissipation, reduced cell and optic fabrication costs, and interconnect flexibility. Arrays of lenses can be fabricated in the form of large area optical sheets via low-cost manufacturing processes. More importantly, the flat physical profile potentially allows leveraging existing silicon module and system components and thus greatly reduces module fabrication and balance of system (BOS) costs. The National Renewable Energy Laboratory (NREL) recently developed a comprehensive bottom-up system cost model that allows evaluating levelized cost of energy (LCOE) for micro-CPV technologies and directly assessing their cost effectiveness. Analyses have shown the strong competitiveness of micro-scale CPV compared to conventional CPV and silicon PV systems.[33]

The micro-scale components further enable new module architectures, such as advanced micro-optic approaches, DNI/diffuse integrated micro-CPV/silicon PV hybrid architecture, flexible PV, waveguide integrated PV, internal tracking, and integrated spectrum management. In particular, integrated hybrid micro-CPV/silicon PV architectures can be utilized to combine high-performance micro-cells and low-cost silicon PV, which would considerably improve power conversion efficiency of silicon devices.[14,27] Furthermore, micro-CPV enables the tracker integration in a module by moving internal subcomponents to continuously capture concentrated sunlight, with displacements of only a few millimeters needed.[34–41] A salient example is the integrated tracking approach from Insolight S.A. using a high acceptance double convex optic and a movable cell-plane. A measured electrical efficiency of 29% was achieved, and the technology is currently being commercially deployed.[42] Such embedded planar micro-tracking CPV can

significantly improve the energy output, making it particularly promising for agrivoltaic, rooftop, and other space-constrained implementations.

While size downscaling can bring in unprecedented performance and cost benefits, new barriers emerge as traditional CPV manufacturing techniques show limited scalability to micro-cells and micro-optics. One challenge is that conventional serial pick-and-place assembly approaches cannot keep up with the massive number of micro-cells and optical alignment precision requirements. On the other hand, traditional large-volume optic fabrication methods limit the achievable minimum dimension, geometry, and architectures of micro-scale concentrators. Furthermore, positioning accuracy of optical elements during the fabrication and assembly processes also poses a bottleneck, which limits the number of optical components that can be utilized, restricting the implementation of advanced multistage concentrator designs at the micro-scale. Since the position and dimensional accuracy of optical elements during the molding process is approximately $\approx 10\,\mu m$, the tolerance to fabrication deviations becomes increasingly tight for micro-optical elements. The fabrication bottleneck, from various aspects, limits the employment of efficient nonimaging optical concentrators in micro-scale PV systems that can bring the concentration performance close to the étendue limit (e.g., by using reflective cones or facets, compound parabolic concentrators, etc.).

As elaborated in the following sections, by leveraging low-cost parallel micro-device fabrication and assembly techniques and new module architectures, recent demonstrations have shown that the scalability hurdles can be overcome with a substantially improved performance and cost advantages. Similar to the evolution of micro-electronics and photonics, "integration" will be the key to transform the original bulk CPV techniques based on discretely assembled macro-components to low-profile flat panels consisting of densely integrated micro-cell and micro-optic arrays. Meanwhile, synergies with other mainstream optical and optoelectronics technologies such as micro-LED displays, flexible displays, LED lighting, micro-electromechanical systems (MEMS), and radio-frequency identification (RFID) will be essential to further growth of the field of micro-CPV.

This review surveys the current state of the art in micro-CPV. A complete overlook of the so-far presented prototypes is given, focusing on components such as micro-cells, optics, and architectures. In addition, we also review the manufacturing methods for assembly/interconnection of micro-cells and manufacturing of optics with the necessary scale and precision requirements for micro-CPV. Published research on improvements of components and manufacturing methods which have not yet made it into a working prototype are also discussed. From the literature research, we identify shared challenges with other industries (automotive, telecommunication, lighting, etc.) and assess technological solutions for a potential cross-linkage with micro-CPV. Many manufacturing and assembly processes are found that could be implemented with ease in a micro-CPV module assembly line, facilitating future scalable micro-CPV module manufacturing while lowering the cost. Two added values that micro-CPV can provide are also discussed, namely hybrid micro-CPV/silicon PV and internal tracking. They are optional but can further the application scope for micro-CPV as they compete with silicon PV. Overall, we aim to present in this review a roadmap to guide the technology selection and development with the goal of expanding and expediting the commercial deployment of micro-CPV technologies.

2. Pioneering Efforts and Current Thrusts on Module/System Development

In this section, we summarize micro-CPV prototype performances published in recent years. In **Table 1**, we include parameters such as concentration, cell size, concentration acceptance product (CAP, Equation (1)), efficiencies, and the type of solar cells and optical system used. Micro-CPV with integrated tracking will be addressed in a later section and summarized in a separate table.

In **Figure 1**, we show the achieved efficiency vs concentration for the micro-CPV prototypes in Table 1, provided that the corresponding publications report both values. From the distribution we can see that most approaches went the conservative way to use a lower concentrations in the range of 100–400X. This results in high electrical efficiencies of over 25% with the highest being 36.5%. This highest optical efficiency is achieved at a concentration a little shy of 180X by the biconvex lenses which are used by Insolight S.A. The prototypes using a hybrid-CPV/silicon PV are found in the middle of the distribution at low concentrations exceeding in many cases the standard micro-CPV approach. These prototypes do not have the maximum attained efficiency results as the global irradiance is used for the efficiency calculation instead of the direct irradiance for the CPV case.

The result with the highest concentration and a very competitive electrical efficiency is from the Semprius micro-CPV module. It is worth noting that this case went through an industrial development phase and developed a commercial product. The product reaches a concentration of over 1000X concentration and outstanding performance with an optical efficiency of over 80% and an electrical efficiency of 35%.[43]

2.1. Identified Challenges

Based on our extensive literature survey summarized above, we identify the key challenges, which must be addressed to enable the success of micro-CPV. Solutions to these challenges are addressed in the following sections.

Manufacturing processes used in conventional CPV, suitable for solar cell units per m² densities of <50, are limited in scalability or simply prohibitive for the micro-CPV solar cell-/optic-scale. For instance, Insolights' micro--CPV- module requires the assembly of 5000 cells and lenses per m².[44] Assembly processes with high precision and low cost are needed for the technology. The micro-LED industry sets a good example, as many challenges are identical.[45,46]

One of the features of the micro-CPV technology is the downscaling of solar cell size for cost reduction. When reducing the cells size, several factors must be considered to avoid electrical efficiency degradation, in particular the perimeter recombination.[47–50] Simulations and measurements have

Table 1. Overview of micro-CPV and hybrid micro-CPV prototypes. The parameters are collected from the references shown in the last column. Images of a few of the prototypes can be found in the following sections. Micro-CPV with integrated tracking will be seen in a separate table in Section 3.7.

Geometrical X	Efficiency η [%]	On-axis opt. eff. [%]	Acceptance Angle (°) @90% opt. eff.	CAP	Cell Size [µm]	Description	Reference
625	34.7	–	–	–	500	3J-micro cells adhered thick aspheric PMMA lens acting as single staged optic. (Panasonic)	[22,69]
300	18	86	2.6	0.79	2300	Si-micro cells (SunPower) with edge surface field, PMMA TIR-R POE with SOE. (Isofoton)	[65] [114]
1111	35	80	0.85	0.49	600	3J-Micro cells SoG POE and ball lenses as SOE. First use of transfer printing and surface mount technology. 3J $\eta = 35\%$ 4J $\eta = 36.5\%$. (Semprius)	[43] [105] [26]
18.4	25.8	65	9.5	0.71	650	3J-micro cells transfer printed, very compact design for space using a reflective inverted compound parabolic lens. (PennStateU)	[122]
13.2	–	82	3	0.19	170	Compact design for space using a reflective glass v-cone tailored edge-ray concentrator. (PennStateU)	[123]
72	12.6	85	3.5	0.52	54	CIGS microcells using photoresin to manufacture the aspheric POE and SOE optics. (IRDEP)	[74]
480	30.4	90	1.65	0.63	970	GaAs single-junction cell surface mounted on injection molded PMMA POE and SOE array. (Panasonic)	[71] [169]
36	10	–	–	–	720	Hexagonal Si-micro cells with a PMMA lens array for POE and SOE. The sandwich is encapsulated with silicone. (Sandia)	[107]
200	–	87	3	0.74	250	2J-micro cells encapsulated with a single aspheric silicone lens array with 83% optical efficiency. (Sandia)	[29,108]
92	35.5	–	–	–	170	4J transfer printed wafer stacked solar cells with a molded glass aspheric array. 4J $\eta = 35.5\%$ projected for 6J $\eta = 38\%$. (NRL)	[84]
1000	–		0.27	0.15	5500	3J-cell with injected PMMA waveguide optic. (Morgan Solar)	[116] [174]
275	29.7	90	0.75	0.22	1000	3J micro solar cell with silicone injected POE and SOE with self-aligning manufacturing. Optical efficiency value is the goal. (CEA)	[170]
1000	33.4		0.5	0.28	600	3J cells with aspheric silicone POE a hybrid dome SOE. (CEA)	[175]
180	36.4	80	–	–	1000	1 mm^2 3J UMM solar cell with byconvex lens, on-axis performance measured and certified by the Fraunhofer ISE. (Insolight)	[176]
180	27.2	79	0.7	0.16	1000	1 mm^2 3J UMM solar cell with bulk molded glass lens array. Eta low due to alignment issues, 33% achievable. (IES-UPM)	[126]
Hybrid Si-PV/CPV							
400	30	90	2.39	0.83	100	Hybrid III–V and Si with wafer-integrated optic (etched V-grooves) as part of a multi-stage optical system with aspheric glass or SoG lens arrays as POE. (MIT)	[109]
100	30.7	87	2	0.35	1000	Micro 3J on bifacial Si cell encapsulated in aspheric silicone POE lenses. (Toyota)	[177]
228	32.7	76	2	0.53	250	Micro 3J on bifacial Si solar cells with a PMMA injected aspherical SOE and Al mirror as SOE. (Sharp)	[106] [111]
740	25.4	–	–	–	170	2J micro cells transfer printed on a bifacial Si cell. Glass molded aspheric lens array. (NRL)	[162]
3.5	30	50	60	1.62	4000	3J cells on Si cells encapsulated in a high acceptance (55°) silicone single lens for car-PV. (Toyota)	[163]
321	34.2	–	0.46	0.14	3000	4J cells on bifacial Si p-PERC cells. With SoG fresnel lenses as only optical stage. (Fraunhofer-ISE)	[178] [164]

shown that losses can be substantial for cells smaller than 500 µm in diameter (corresponding to a perimeter to area ratio of ≈ 80 cm^{-1}), as can be seen in **Figure 2**A. Another factor is the material loss during wafer dicing when singulating the solar cells. Standard technologies such as diamond sawing and laser ablation have lane widths (lost area between active dies) in the micron range[50–52] (Figure 2B). These technologies also contribute to the aforementioned perimeter recombination losses for solar cells, by causing mechanical defects during the dicing process.[48] In addition, cell assembly and interconnection at the micro-scale raise a cost issue. Due to the large area and high density of dies, the assembly cost rises exponentially
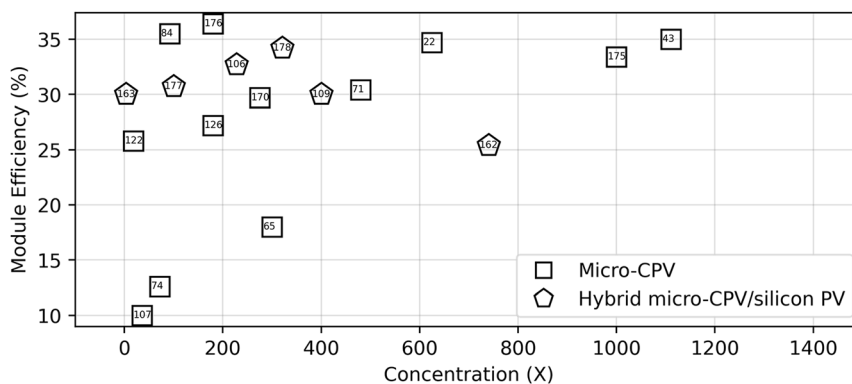
Figure 1. Efficiency versus geometrical concentration ratio for the prototypes in Table 1. They are divided into two groups: micro-CPV with squares as markers and hybrid micro-CPV/silicon PV with pentagon markers.
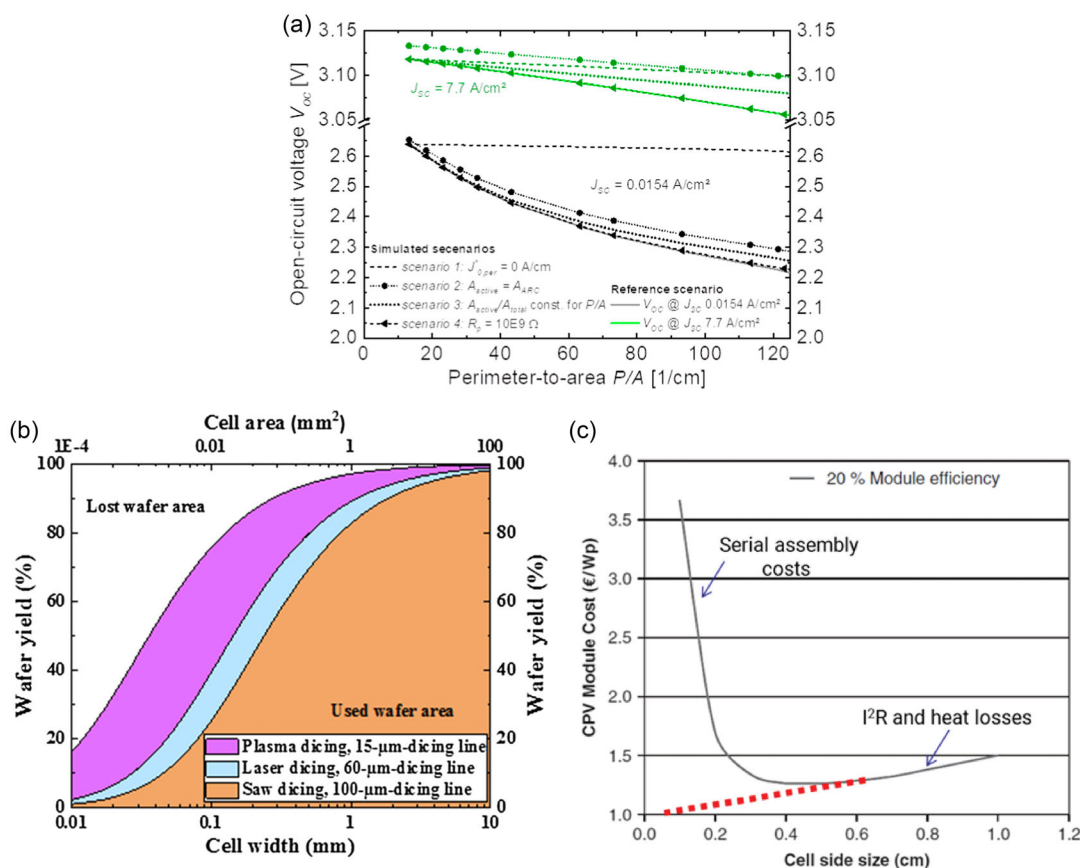
Figure 2. a) Effect of perimeter recombination for solar cells below 500 μm in diameter or side length (P/A ≈ 80 cm^{-1}), showing reduction of open-circuit voltage loss which has a negative effect on the efficiency. Reproduced with permission.[49] Copyright 2021, Elsevier BV. b) Conventional dicing technologies for various sizes of dies indicating that plasma etching is best suited for small dies such as micro solar cells. Reproduced with permission.[50] Copyright 2021, Institute of Electrical and Electronics Engineers (IEEE). c) Assembly costs predominates CPV module cost for small cells, where the dashed red line shows the ideal case for micro-CPV. Reproduced with permission.[53] Copyright 2017, AIP Publishing.

(Figure 2C).[53] The die interconnection has been traditionally carried out with wire bonding. This method is prohibitively expensive for micro-solar cells as contact areas such as pads and busbars must be downscaled proportionally to avoid increasing the shading factor.[50] Alternatives to wire bonding are necessary.[54]

The optical performance can be enhanced in micro-CPV benefitting from the short optical paths, but manufacturing of very small units on large areas is a challenge. For very thin optics, high-throughput manufacturing methods such as roll-to-plate or roll-to-roll represents an attractive low-cost manufacturing method,[44] although achieving good optical quality remains

difficult.[55] Micro-CPV allows for the use of novel optical designs, which were previously not viable, yet machining of optical molds for micro-optics is not trivial. High precision with good surface finish is needed, although in most cases the viable types of machining methods are area constrained.[56] In addition, aligning cell-optic at a micron scale is difficult.[57,58] For this case, internal tracking enabled by the small size of the optics offers an intermediate solution as the implementation of an actuated solar cell or optical plane increases the complexity of the module.[42]

The next section scrutinizes potential solutions for these challenges in the context of their applicability, constraints, and advantages for micro-CPV.

3. New Enabling Technologies for Micro CPV

3.1. Micro Solar Cells

In micro-CPV, the cell size is reduced, which comes with electrical efficiency losses due to several issues. To obtain highly efficient, sub-mm sized solar cells certain requirements must be met: operation under high-intensity light flux, reduced perimeter recombination losses, low shading losses without incurring excessive resistive losses, compatibility with single-sided contacts, and low material loss due to die singulation. In the development of micro-solar cells, we can mention works from the Naval Research Laboratory (NRL),[59–61] Sherbrooke University,[50] Instituto de Energia Solar (IES-UPM),[62] Fraunhofer ISE,[49] and Sharp.[63]

Perimeter recombination is influenced by the perimeter area of a solar cells' active layers,[47] simulation studies have shown significant losses at low concentrations.[62,64] The conclusion is also consistent with the analysis of Espinet et al. on perimeter recombination, higher current densities (under high concentration) ameliorate the impact of the perimeter losses.[47] Perimeter recombination causes the loss of open-circuit voltage, which directly reduces the electrical efficiency of the solar cells, as is evident from Figure 2A.

Passivation of the lateral surfaces has been implemented for silicon micro solar cells. This passivation is referred to as edge surface field (ESF),[65] yet for multijunction solar cells this approach is complicated given different semiconductor materials are used in the stack. Still, a successful approach has been shown using the antireflection coating as lateral passivation and insulation for tandem solar cells.[50] Other means to avoid the perimeter recombination includes adding a heterojunction as a window layer as suggested by[62] or reducing the thickness.[49,50]

Plasma etching is used to avoid material loss when dicing the cells. This technique can reduce dicing widths from >80 μm to 10 μm and lower depending on the thickness of wafer and allow versatile designs of solar cell shapes[50–52] (Figure 2B). Plasma dicing has other benefits including better mechanical properties, which result in a higher process yield, and improved sidewall surface quality, which has been connected with reduction of perimeter recombination in solar cells.[50] LEDs that also show perimeter recombination for very small devices <10 μm[66] caused by sidewall damage during singulation.[67] Plasma etching is necessary for high-performance devices for both industries. Furthermore, throughput improvement and cost reduction have been associated with small and thin dies given

a constant dicing speed.[51] Thin dies can also improve the open circuit voltage (V_{OC}) of solar cells on germanium substrates.[68]

When it comes to mitigating the shading factor for small cells, a solution is to move the contacts to the back side using metal interconnects[69] or via metal wrap-through contacts (**Figure 3**A).[48,52,70] These one-sided contact solar cells enable self-alignment during the soldering process, as is illustrated in Figure 3B for front contactable solar cells.[71]

Another approach worth mentioning is CIGS solar cells. Micro CIGS cells can be manufactured directly on low-cost substrates with high precision.[72,73] First attempts to manufacture a micro-CPV module with CIGS solar cells have already been attempted.[74] These attempts started out with a top-down approach, the removal of material to manufacture the micro-solar cells. This concept is prohibitive as material is lost. Currently, work is being done on the bottom-up approach, with which no material is lost as shown in **Figure 4**. This approach is very low costs and avoids later assembly costs. The positioning tolerances are very good as photolithography is used. The limitation is the efficiency of CIGS solar cells manufactured in this manner, which is still to exceed 20% efficiency.

3.2. Solar Cell Assembly

The assembly of a vast number of cells on a large area, thousands per m², is essential for micro-CPV. This is a challenge which is difficult to address with conventional technologies used for CPV such as pick-and-place or manual assembly. Parallel assembly of the solar cells can leverage different technologies, many of which having been developed for the micro-LED industry: micro-transfer printing, chiplet printing, fluid self-assembly (FSA), and others. The most promising approaches are listed in **Table 2**. Different variants of the technologies will be discussed later.

3.2.1. Fluidic Assembly

Fluidic assembly or FSA uses shape matching or capillary forces to position and assemble dies. An example for shape matching was developed by the company eLux which assembles micro-LEDs using a film with cavities submerged in a liquid.[75] Other approaches working under the same principle (cavities, forces and shape recognition) are discussed in ref. [76]. Capillary forces for FSA have been studied extensively and systems with industrial potential are available for assembly of LEDs, with state-of-the-art results from a collaboration of the TU Ilmenau with the University of Minnesota. The results of their collaboration where first presented for flat substrates.[77] Then, a functional roll-to-roll system was demonstrated in ref. [78]. This FSA system used solder bumps on a flexible film to position and fix the dies in place, this can be seen in **Figure 5**. The dimensions of the LED dies used in the roll-to-roll FSA are similar to micro-CPV solar cells, and the solder bumps tailored for this process also meet the thermal budget for micro-cell assembly, which involve a low temperature of 75 °C for the FSA process.[77] Single junction 1000 mm sided GaAs solar cells were successfully assembled using FSA to create a micro-CPV module. Up to 256 solar cells could be assembled at the same time on a 40 × 40 mm² PCB.[79]

(a)

(b)
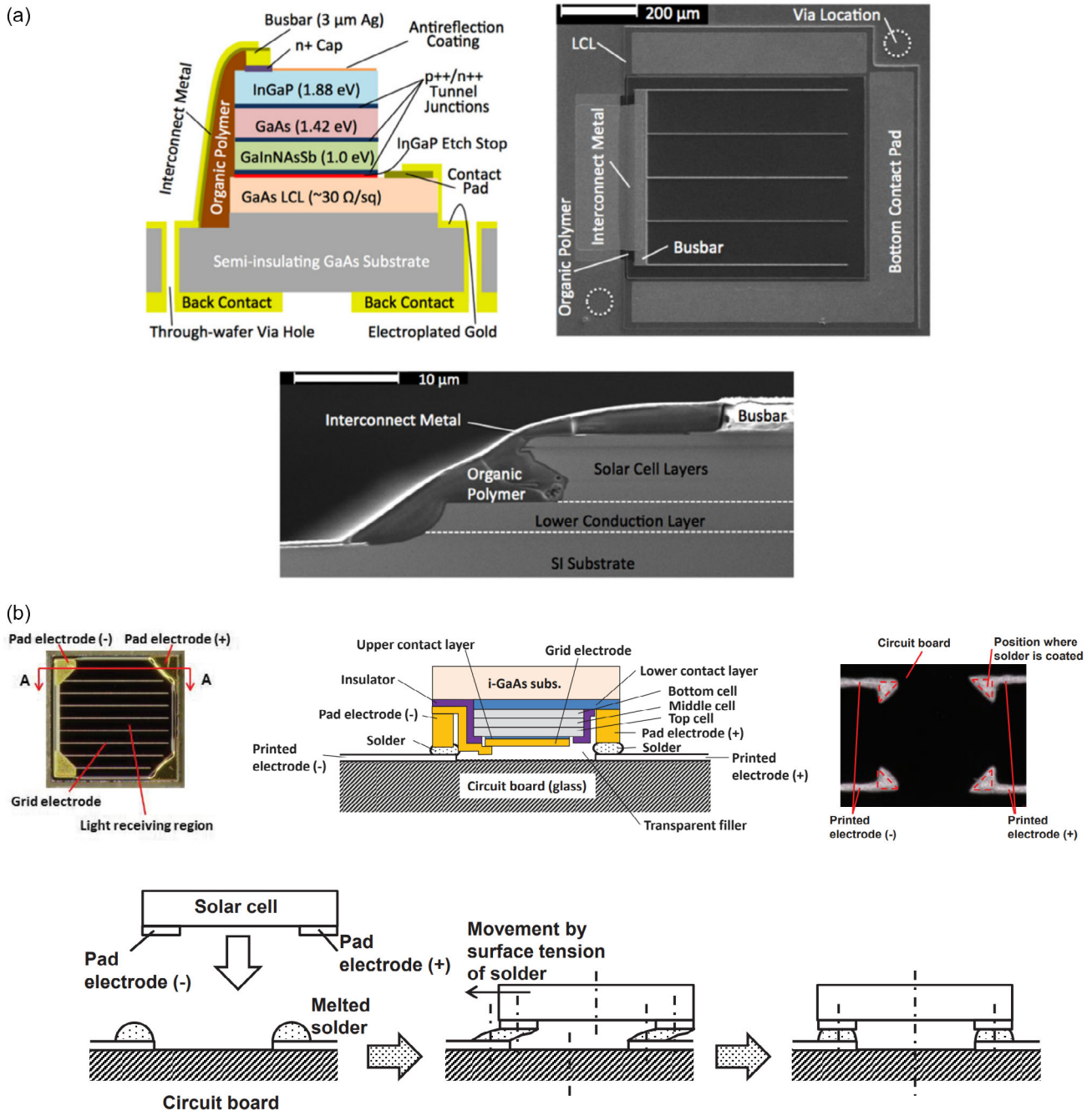
Figure 3. a) Through-wafer via-hole contacts for backside-only interconnection of solar cells is an attractive option for micro-CPV. Bringing both contacts to one side comes with an initial investment for further optimization of the processing of the solar cells. Yet, the final assembly of the small devices is easier. Reproduced with permission.[69] Copyright 2014, AIP Publishing. A good example can be seen in (b) where self-alignment compatible micro solar cell with front contact interconnection is seen being soldered on a circuit board. Reproduced with permission.[71] Copyright 2017, AIP Publishing.

3.2.2. Chiplet Printing

Developed by PARC, this process assembles dies on a desired array pattern using electrostatic forces applied through spiral-shaped electrodes (on a Xerographic μ-assembler). Once the dies are arranged, they are transferred with a roller onto the final substrate and electrically interconnected. This process, which is described in ref. [80] (see **Figure 6**), leads to the possibility to assemble different micro-solar cells with different performance characteristics on the same substrate. Results with assembled solar cells and LEDs are elaborated in ref. [81]. For micro-LEDs, this is a solution for assembly of different dies for the needed RGB colors, and for solar cells this approach can be used for lower performing optics (large focal
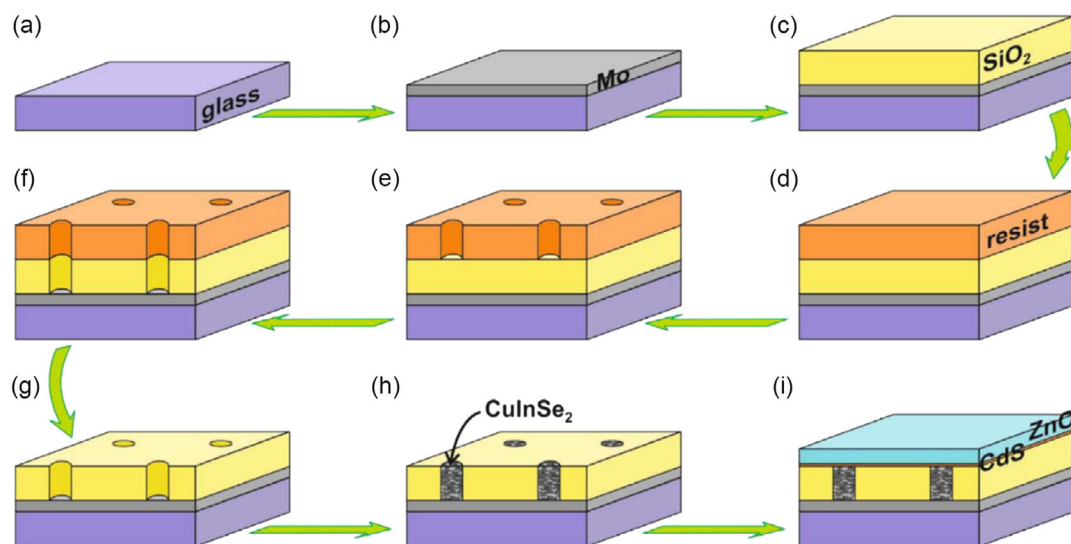
Figure 4. CIGS is a solar cell technology, which allows for a very local manufacturing on a base substrate. Avoiding later assembly costs and allowing for a much alignment higher precision with the tolerances of the photolithography process used. Here the CIGS micro solar cells fabrication process is shown from (a–i). After the photolithography and etching steps (d), the solar cells are deposited locally using electrodeposition and a Se atmosphere annealing (h), and then finished with a CdS chemical bath deposition and ZnO sputter for the double window layer. Reproduced with permission.[72] Copyright 2017, Elsevier.

Table 2. Micro-LED assembly methods following[75] with additional data from the references listed in the last column.

Technology	Company	Transfer Rate Million [h]	Price [$ m^{-2}]	Precision [μm]	References
Fluid Assembly	eLux	50	–	<0.2	[78,179]
Elastomer Stamp	X-Celeprint	1	0.16	<5	[101,180]
Roll-Stamp	PARC/Xerox	3600	15	5	[80]
Laser Transfer	Uniqarta	>100	–	1.8	[181]

spots due to low concentration). For the region where the optic is performing well, high-power solar cells can be used and for the lower performing areas low-cost solar cells can be assembled.

3.2.3. Micro-Transfer Printing

Industrial deployment of micro-transfer printing was started by Semprius[43] and continued by X-Celeprint and Microprince. Many different institutions such as the X-Fab are active in this field.[82] The key feature of micro-transfer printing is the use of an elastomer stamp to transfer the dies.[83] This approach is based on Van der Waals forces, which can be controlled by the speed and direction of the peeling action with the elastomer stamp, this is illustrated in **Figure 7**. The dies are undercut-etched and released from the source wafer using the stamp and then transferred to a final substrate with already patterned adhesive/solder for electrical interconnection.[82] This technology is used for different types of opto-/electronic III–V devices including micro-CPV solar cells for the manufacturing of mechanically stacked four (or more) junction solar cells.[84,85]

In **Figure 8**A, an illustration of a five junction solar cells is shown. These solar cells are manufactured by stacking, which is done by transfer printing a two- and three-junction solar cell grown on different substrates, obtaining the best performance for each solar cell.[85] Attempts are also being made in adapting this process to a roll-to-roll production line, using rollers made from elastomeric materials with surface texture to impart directional controllable adhesion.[86] As with chiplet printing, this approach can also be used for the assembly of multiple devices close to each other with high precision. This is shown for the laterally arrayed micro-cells in conjunction with spectral splitting optics developed by MIT[87,88] seen in Figure 8B.

3.2.4. Other Transfer Technologies

Laser-induced forward transfer (LIFT) is another massive selective transfer method. This process is used for GaN LEDs grown on sapphire substrates. Laser beam irradiation causes delamination of the dies from the carrier substrate and further propels the detached dies toward a receiving substrate, the approach is described in the following publications.[75,89] Solar cells can also be grown on sapphire and transferred as shown in ref. [90], though their electrical performance is currently low. Electrostatic transfer arrays developed by LuxVue uses specialized electrostatic transfer heads with which the dies can be selectively picked up and released.[45] This technology can be applicable for micro-CPV solar cells since dimensions and characteristics are similar as for the micro-LEDs which have been used in ref. [45]. In magnetic transfer arrays developed by EOSRL-ITRI, an electromagnetic device selectively picks up one or multiple micro-dies onto a target substrate.[45] This method is similar to the previously mentioned electrostatic transfer approach, this process is compatible with micro-solar cells as well. A throughput of
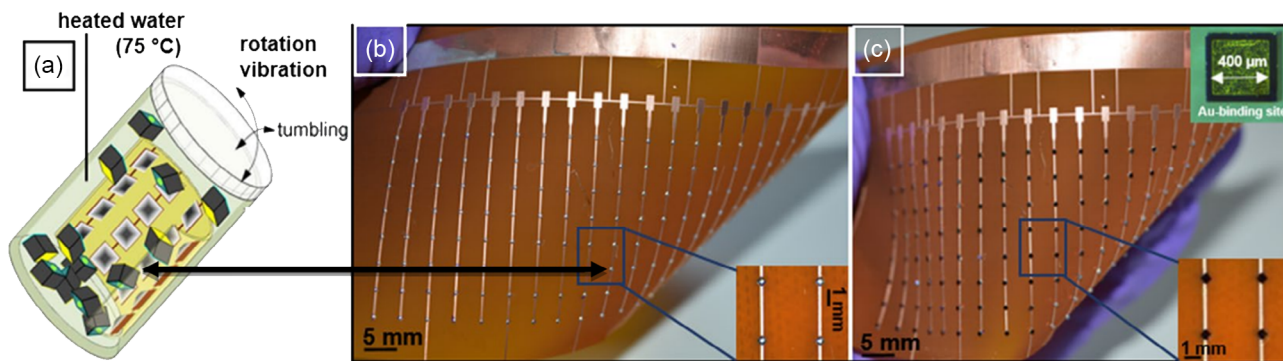
Figure 5. The collaboration between the TU Ilmenau and the University of Minnesota lead to a FSA system tailed for the assembly of 400 μm LED dies on a flexible substrate. a) The dies and flexible substrates are incorporated in tumbler filled with heated water. They are kept under constant movement until all the dies adhered to the solder bumps seen in (b). When the temperature is lowered the dies solder in position. c) The resulting substrate with soldered micro-dies with a high yield of >90%. This high yield makes this a viable approach for the industry and an attractive solution for micro-CPV which uses similar sizes of dies. Reproduced with permission.[77] Copyright 2019, Springer Nature Limited.
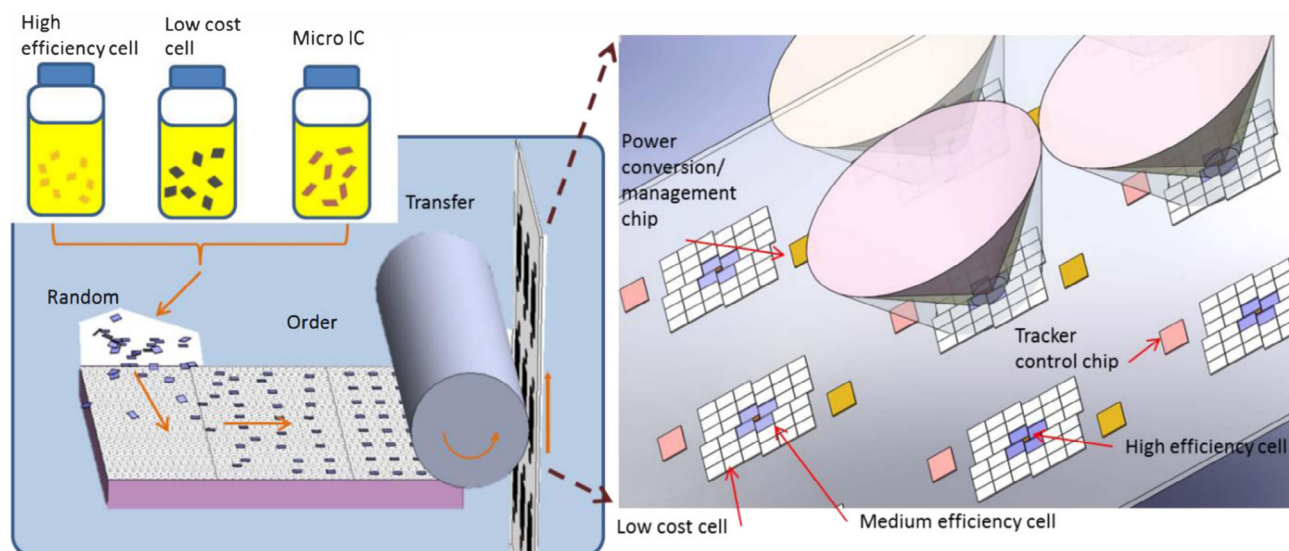
Figure 6. Chiplet printing using a roller. The concept is printing multiple micro solar cells with various electrical efficiencies in one lens focal spot. Taking advantage of an inhomogeneous irradiance mesh to homogenize and therefore maximize the electrical output. Reproduced with permission.[80] Copyright 2015, Insitute of Electrical and Electronics Engineers.

10 thousand dies per hour has been reported for magnetic transfer in ref. [91]. The Korean Institute for Mechanics and Machining (KIMM) developed a roll-base transfer technology.[45] This process is similar to the chiplet printing method for solar cells developed by the company PARC.[80]

Many of the technologies mentioned in this section are tabulated in **Table 3** from.[45]

3.3. Interconnection of Cells

In micro-CPV, the number of solar cells per area increases to thousands of cells per m^2, well beyond the limits of technologies used in traditional CPV such as tab soldering and wire bonding. Interconnection of solar cells on this scale while maintaining a competitive cost is therefore a major challenge. Micro-LED arrays face similar challenges in electrical interconnection, and several mass transfer technologies are being explored for micro-LEDs, a good collection can be seen in the following article.[75] Most of these approaches are also applicable to micro-CPV and will be discussed in this section. The goal is to reduce the cost to \$50–100 m^{-2} for assembly and interconnection as suggested in ref. [46]. Interconnection alone should reach costs as low as \$3–4 m^{-2} for viability for micro-CPV, this goal leaves margin for the high precision assembly. This cost is achievable as described in ref. [54]. Candidate solutions include metallization via evaporation, a standard micro-processing step; conductive ink printing, an approach more suitable for large areas; chip-on-board (COB) combined with printed circuit boards (PCBs); and overcell contacting using transparent conducting coatings on the die. These technologies are compared in **Table 4** and further discussed later.
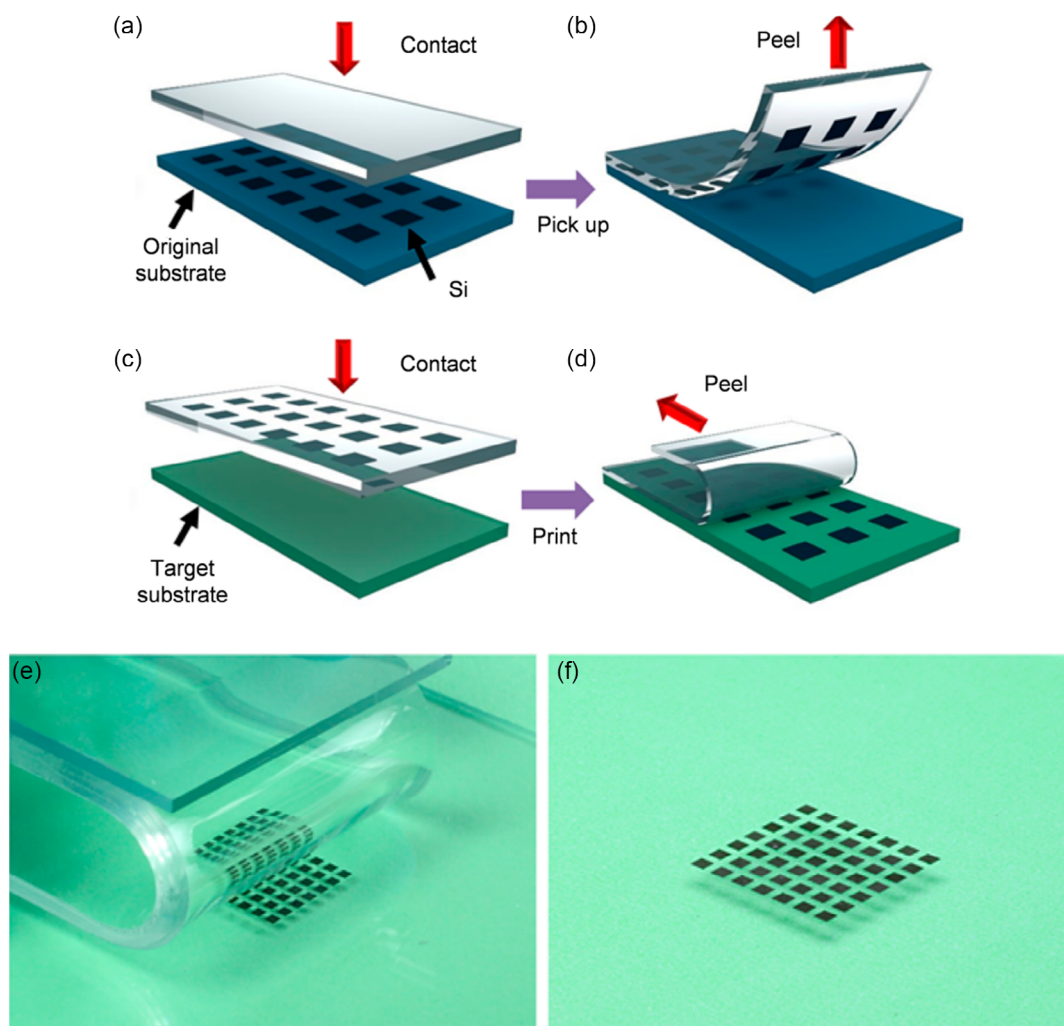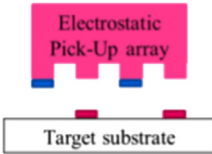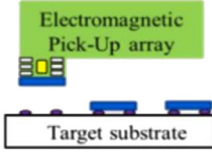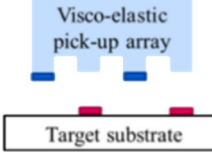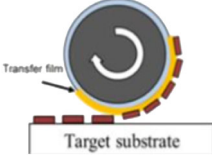
Figure 7. a–f) Micro transfer printing using an elastomer stamp process. Beside with micro-LEDs this assembly technology has already been demonstrated with solar cells, by Semprius Inc. and by the Naval Research Lab. Currently, the technology is being developed for industrial application from X-celeprint and Microprince. Reproduced with permission.[83] Copyright 2016, American Chemical Society.
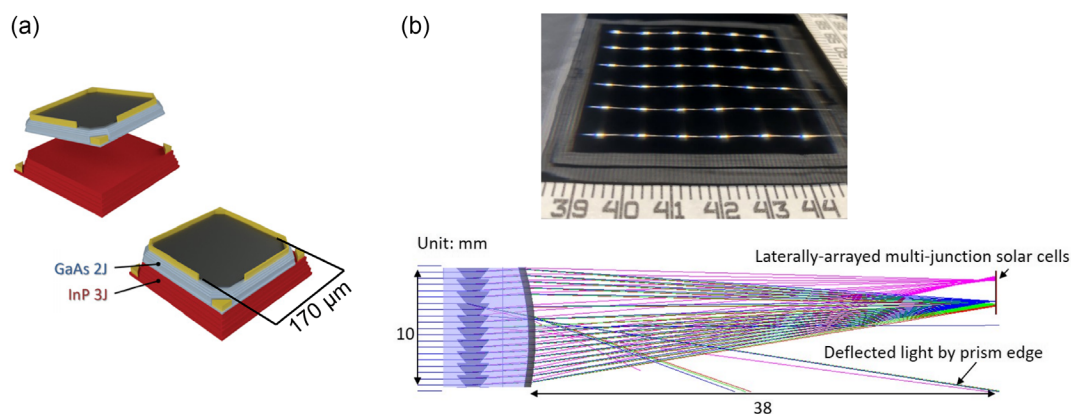
Figure 8. a) Shows the structure of a mechanically stacked 5 J micro solar cell; Reproduced with permission.[85] Copyright 2019, IEEE. b) Spectral splitting optics for laterally arrayed multijunction solar cells. Both these micro solar cell technologies (A&B) are manufactured by very high-precision transfer printing, the precision necessary for these technologies is <5 µm. Reproduced with permission.[87] Copyright 2019, Insitute of Electrical and Electronics Engineers.

Table 3. Showing transfer printing technologies currently used for micro-LEDs. Reproduced with permission.[45] Copyright 2018, MDPI.

	Company	Principle	Description
Electrostatic array	LuxVue		The transfer heads are divided by the dielectric layer to form a pair of silicon electrodes, which are positively and negatively charged, respectively, before picking up the target LED.
Magnetic array	ITRI		Micro-LEDs are adsorbed and placed by the electromagnetic force generated by the coil.
Elastomer stamp	X-Celeprint		The pick-up and transfer processes are aided by the Van der Waals forces between the viscoelastic elastomer stamp and the solid micro-LEDs
Roll to plate	KIMM		A roll-based transfer technology for transferring nanoscale objects from a donor substrate to a target substrate with high yields and productivity

Table 4. Interconnection methods for micro-CPV.

Technology	Institute/Industry	Area	Price [m^2]	Precision [µm]	References
Metal evaporation	NRL/micro-CPV & LED	Small	Very high	<1	[84,92]
Wire bonding	Micro-CPV scale	Medium	≈ $500 (High)	50	[54,182]
Interconnective (screen) printing	UPM/micro-CPV & LED	Large	$3–4 (Low)	20	[54]
Interconnective (aerosol) printing	Joanneaum/micro-LED	Medium	Medium	<100	[94]
One sided interconnection	Panasonic/micro-CPV & LED	Large	Medium	10	[71]
Chip-on-interposer	Insolight, Semprius/micro-CPV	Large	Medium	10	[44,101]
Overcell contacting	Micro-LED	Large	Low	–	[102]

3.3.1. Metal Evaporation

Physical vapor deposition (PVD) and lithographic patterning of metals usually apply to small-area devices given the steps' relatively high cost. This approach has been used for small-area micro-LED screens[92] and micro-CPV prototypes.[84]

PVD has its benefits when applied to complex interconnection layouts, such as for mechanically stacked five junction solar cells used by NRL. As both stacks have different current outputs, a complex interconnection scheme is designed to maximize the total power output. This interconnection method uses lithography steps and allows for these complex interconnection schemes as seen in ref. [93]. In addition, the resists used in the lithography step permit electrical insulation of the edges of the solar cells, avoiding short circuiting. A type of self-alignment process is also possible with lithography, this can be used to form electrical insulation and small channels on micro-CPV solar cells in one step. These

channels are then filled with conductive silver paste for interconnecting solar cells. This approach was shown for interconnecting 256 solar cells on an area of $40 \times 40\,\text{mm}^2$ in ref. [79].

A concern for the evaporation technology is the high cost, lithography on large areas is expensive and if the process is not optimized valuable metals are wasted.

3.3.2. Interconnect Printing

Conductive printing is a technology easily applicable for large areas. Different printing approaches can be used such as screen, inkjet, electrohydrodynamic (EHD), aerosol, gravure, and roller printing among others.[55] These printing technologies are shown in **Figure 9**. The printable substrates vary from rigid glass/plastics to flexible/stretchable polymers. These printing techniques are used in an abundant number of technologies from the front- and back contacts of Si solar cells,
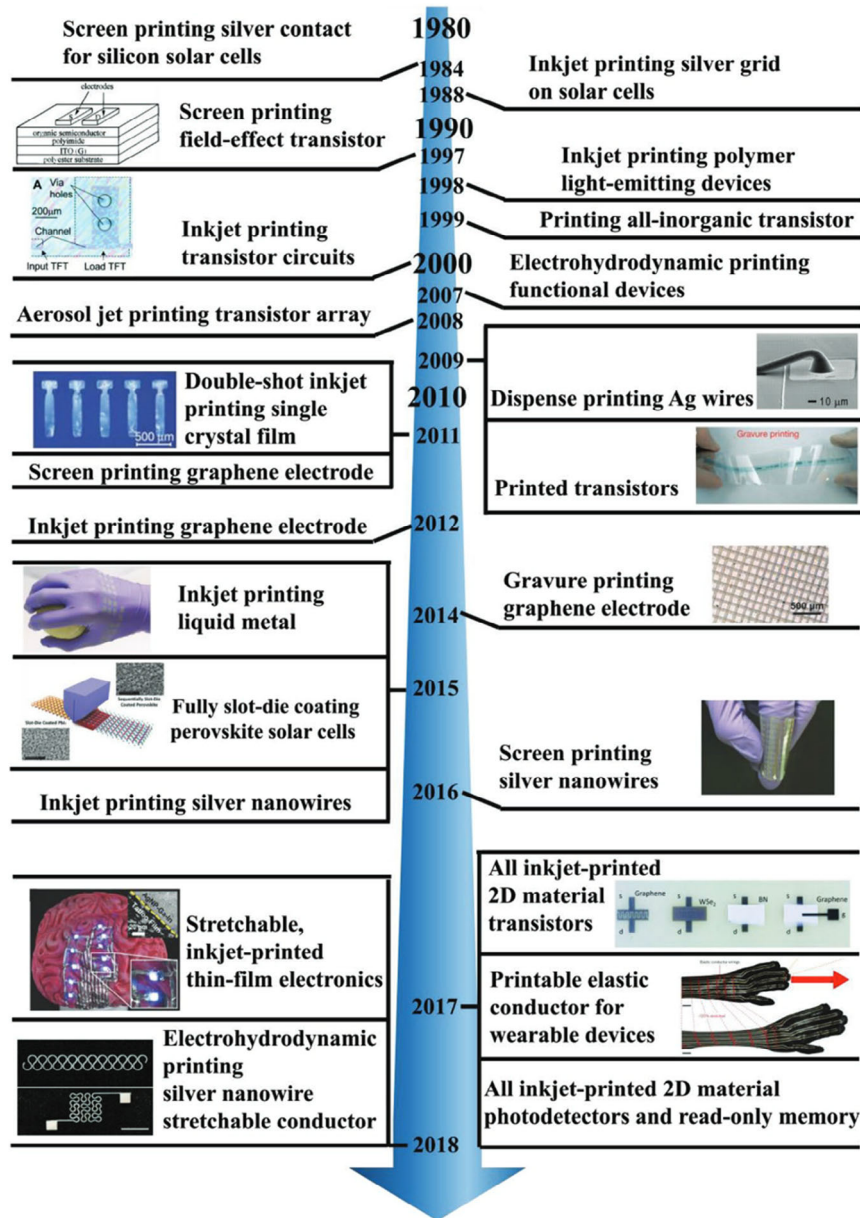
Figure 9. Timeline showing the large number of conductive printing technologies developed throughout the years in the semiconductor industry. Screen printing is the standard technology for printing the front- and back-contact of Si solar cells. For micro-CPV, the silver nanowire inks developed in 2015 come in question for the interconnection of solar cells. Reproduced with permission.[95] Copyright 2019, John Wiley & Sons Inc.

the interconnection of micro solar cells, printing of functional sensors/transistors, perovskites, radio-frequency antennas, and stretchable electronics.

What makes these technologies appealing is their broad applications across different industrial sectors such that micro-CPV can take advantage of the technical expertise and infrastructures developed for other applications. A mandatory requirement for micro-CPV is the capability of printing not only conductive materials but also dielectrics needed for the lateral isolation of dies and tracks. A good example is the work in ref. [94], which employed aerosol jet printing for LED-die contacts on a PCB to avoid wire bonds. The LEDs used both front and back contacts,

where the back contact was directly soldered on the PCB. A dielectric layer was first printed on the front side, followed by printing of a silver conductive ink to interconnect the frontside contacts as depicted in **Figure 10**A. Aerosol jet printing was used leveraging its high precision and also because the same technology was used for the deposition of phosphor layers on the same LED dies for color conversion.

Electrohydrodynamic (EHD) printing can process complex structures, from drop-by-drop nanowires to high-aspect-ratio walls.[95] EHD printing is based on electrohydraulic forces to propel ink through a nozzle, and the result thus depends on the nozzle size and ink viscosity.
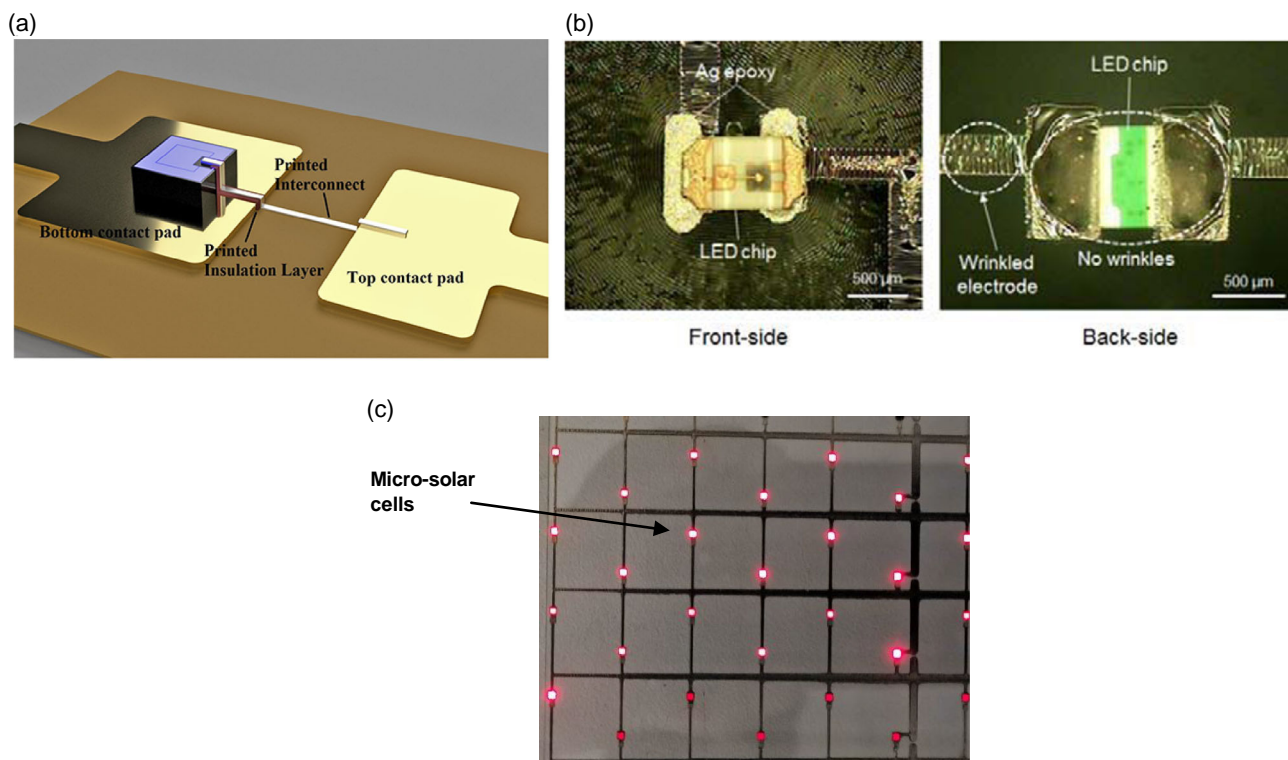
Figure 10. a) An alternative to wire bonding for LEDs using jet printing of an insulation layer and conducting layer to interconnect a die. Reproduced with permission.[94] Copyright 2016, Society of Photo-optical instrumentation engineers (SPIE). b) Printed electrodes for use with the chip-on Interposer technology, in this case on flexible and stretchable substrates. Reproduced with permission.[98] Copyright 2017, Society for Information Display. c) A section of a screen-printing interconnected 1 mm² multijunction solar cell array. Reproduced with permission.[54] Copyright 2022, Elsevier.

Screen and gravure printing are promising printing technologies for micro-CPV because they can be scaled up to large areas > 1 m² with a high resolution of 70 μm line widths achieved in the following publications.[95,96] Smaller line widths of ≈ 20 μm are achievable but are limited to a total area of ⌀450 mm (18 inch) or less since lithographically patterned silicon wafer-based stencils have to be used.[97] For micro-CPV, screen printing can be used to directly contact solar cells with conductive inks, although cell perimeters need to be electrically insulated prior to contact printing. This method is further described in ref. [54], and the result can be seen in Figure 1C. The technology can also be used to print large-area flexible or rigid substrates. On these reflow soldering can be used to directly solder back-contactable chip-on-interposers LEDs. This process on flexible substrates is described in ref. [98] and shown in Figure 10B. Through-via contactable solar cells with both contacts on the back side, mentioned in ref. [52], could also be used with this interconnection approach.

An early-stage technology that could be used for interconnecting micro solar cells is pressure-activated interconnection during transfer printing. In this process, micro-electrical connectors (jumpers) are first manufactured with MEMS technologies on a silicon wafer and then transfer printed onto contact pads. This technology is being developed for micro-LED displays by the company X-Celeprint Inc, it is described in ref. [99].

3.3.3. Reflow Soldering on Micro-Solar Cells with Single-Side Contacts

Several parallel interconnection methods are available for soldering solar cells with one-sided contact pads, all of these have been mentioned previously and can be seen in the publications.[48,52,71] Reflow soldering is also used in combination with other interconnection technologies such as the previously described interconnect printing. Placement of the cells can be done by R2R fluid assembly or transfer printing. Reflow soldering can be subsequently used to interconnect solar cells with high resolutions down to 10 μm, achieved by Panasonic for their micro-CPV module prototype.[71] This precision is sufficient for the micro-CPV technology when solar cells larger than 100 μm in side are used.

3.3.4. Chip-On Interposer/Chip-On Board

Chip-on interposer (COI), also sometimes called chip-on board (COB), is a technology widely used in electronics and now also for micro-LEDs and micro-CPV solar cells. A schematic of these devices can be seen in **Figure 11**A. The concept involves bonding the dies on a PCB using standard manufacturing technologies such as wire bonding and pick-and-place. In addition, optical
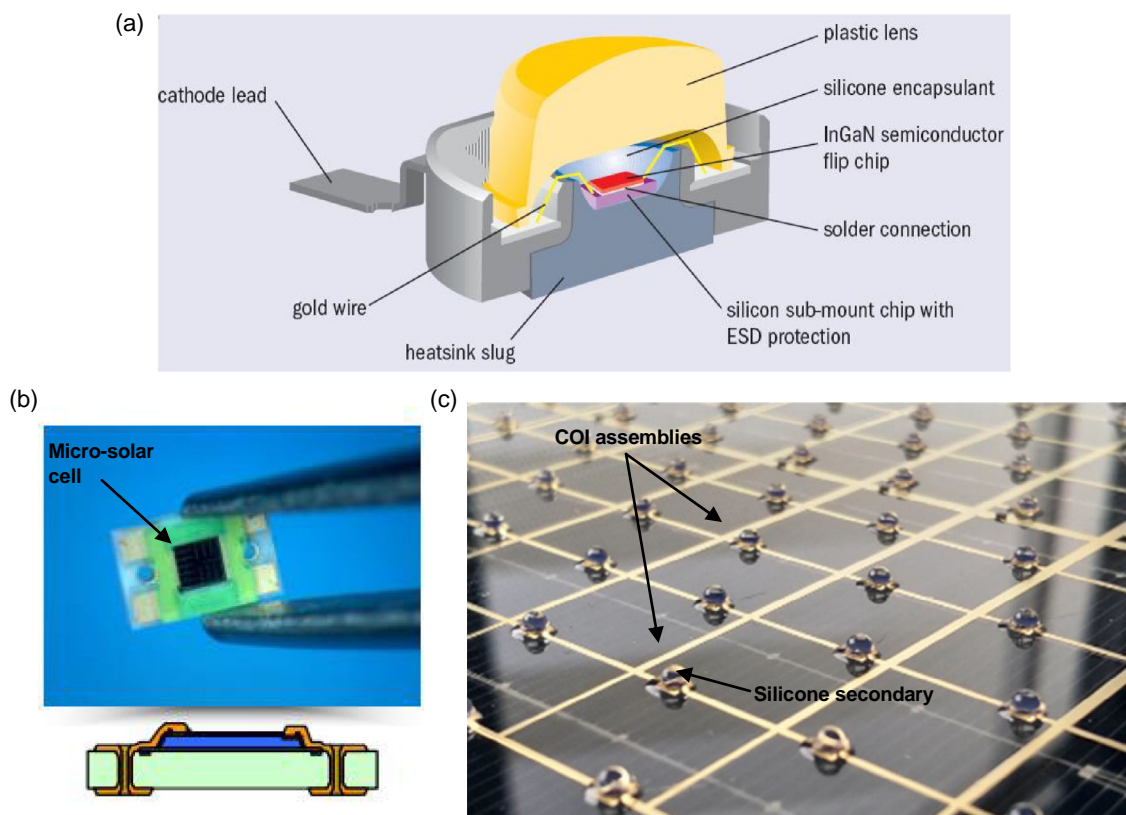
Figure 11. a) A chip on interposer (COI) assembly which is common in high power LEDs, Reproduced with permission.[172] Copyright 2006, SPIE. b) Semprius surface-mount interposer for 600 μm sided solar cells. Reproduced with permission.[101] Copyright 2014, IEEE. c) Insolight's hybrid approach with COIs reflow soldered on glass substrate with encapsulated silicon PV solar cells underneath. These COIs have an over molded silicone secondary optical element. Reproduced with permission.[44] Copyright 2020, John Wiley & Sons, Inc.

elements can be directly over molded on the chip.[100] Assembly lines for COI already exist in the LED industry.[98]

Semprius used this approach for their 600 μm micro-solar cells, naming the technology surface-mount interposer,[101] as shown in Figure 11B. The interposer is a surface-mount substrate where the cells are first attached and then wire bonded. Insolight is taking advantage of this approach as seen in Figure 11C. A challenge for micro-CPV is the tight alignment tolerance between the primary optics and COIs on large-area substrates, which can be relaxed via the integration of a secondary optical element (SOE) onto the die in a COI assembly.[44]

In Figure 11A, a more complex COI approach is depicted involving heat sinks and plastic optics. The optics can be alternatively made from over molded silicone. The die interconnection was carried out traditionally with wire bonding, although lately printing methods have gained ground.[94] Both electrical contacts are placed on the back side of the COIs, which facilitates transfer onto printed interconnection circuits, e.g., flexible substrates previously seen in Figure 10B.[98]

3.3.5. Overcell Contacting

Overcell contacting using transparent conductive layers such as oxides, graphene, metal nano-wires, or other transparent conductive layers have been adopted for low-concentration CIGS solar cells in refs. [72,74]. In LEDs, transparent conductive layers are being used as electrodes for the dies. A conductive material candidate of particular interest is graphene, which can be used for visible and UV LEDs[102] as well as for multijunction-solar cells[103] given its excellent transmittance in the UV and visible light spectral region. Silver nanowires have also been proposed for LED interconnection in ref. [104]. The overcell layers are amenable to gravure printing (graphene) and aerosol printing (nanowires).

The transparent contacts can eliminate traditional metal contact pads, bus bars, and metal fingers on the cell front side, thereby mitigating shading losses. For this application, a transmittance value of 98%-99% with a low electrical resistance of 20–30 $\Omega\,sq^{-1}$ is necessary.

3.4. Advanced Optical Approaches for Micro-CPV

Size downscaling enables many new micro-optical architectures to be applied to micro-CPV.[53] These different approaches can lead to high optical performance or cost reduction capitalizing on high-throughput manufacturing methods. **Table 5** reviews various optical designs proposed for micro-CPV.

Table 5. New optical architectures for micro-CPV.

Technology	Company/Institute	Acceptance [°]	Concentration (X)	CAP	Price	Challenge	Reference
Multistage with refractive primary	Sandia/MIT	2.2	400	0.76	Low	Alignment	[109]
Multistage with refractive primary	Semprius	<1.5	500–1000(SOE)	0.82	Low	Acceptance angle	[107]
Single stage with refractive primary roll-to-roll	IMDEA/IES-UPM	0.6	180	0.14	Low	Durability material	[128]
Single stage coupled to solar cells	Nagaoka UT	1.5	200	0.37	Medium	Concentration	[111]
Total internal reflection (TIR)	Isofoton	2.5	250–500	0.69	Medium	Complex molding	[65]
TIR-all dielectric	IES-UPM/MIT	1	1000	0.55	High	Complex molding	[112]
Refractive + reflective	PennStateU	9.5	18.5	0.71	Medium	Molding large area	[122]
Spectral splitting	MIT	–	–		Medium	Complex	[87]
Waveguide	Morgan Solar	<1	1000	0.55	Low	Aceptance	[116]

### 3.4.1. Multistage with Refractive Primary

Two-stage optics with a refractive primary optics (POE) is the most common approach for conventional CPV since adding a SOE enhances the CAP. In micro-CPV this approach has been also widely proposed by several authors. Fresnel lenses, which incur inherent losses due to draft angles and tip rounding in the lens facets, may still be applicable but not strictly necessary for the case of micro-CPV thanks to the scaling-down of overall thickness. Reducing the number of facets would enhance performance, while a higher facet number would reduce material volume and benefit the cost.

Semprius modules used silicone-on-glass (SoG) lenses together with a ball lens SOE to achieve a concentration of 1111X on 600 µm sided solar cells with an optical efficiency of 80%.[105] Panasonic proposed injection molded PMMA Fresnel lenses for their micro-CPV system with a concentration of 200X,[106] which increased to 480X with a SOE.[71] In their prototype modules, they showed that micro-CPV enabled them to process both the POE and SOE using injection molding.

Sandia Labs and MIT developed a concentrator module comprising a three-stage optical system. Various iterations were published. The first prototype involves a molded PMMA array of micro-lenses concentrating sunlight onto hexagonal silicon solar
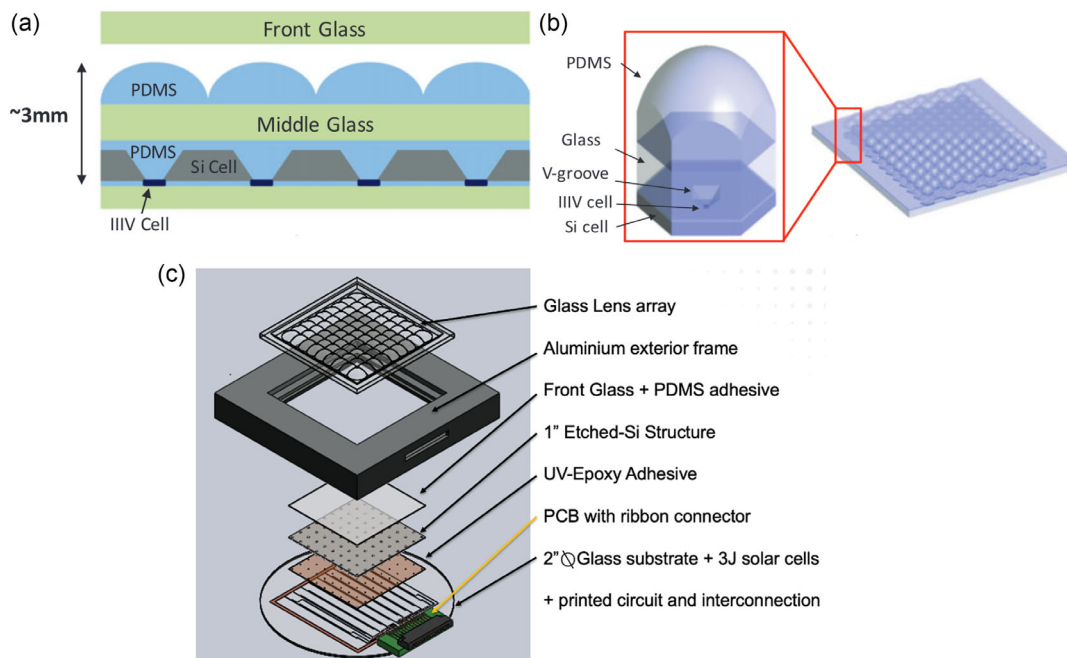
Figure 12. a) A cross-section and b) 3D view of a MIT developed complex optical system for micro-CPV. This system can achieve concentrations exceeding 1000X and is composed of multistaged glass/PDMS optics and etched inverted pyramids (labeled as V-grooves) into a silicon wafer as secondary optical element. Reproduced with permission.[109] Copyright 2018, John Wiley & Sons, Inc. In further iterations, the design was simplified to use a glass molded optical array as primary optical element and the V-grooves as secondary. A schematic of how the final prototype looks like can be seen in (c). For future works the silicon wafer is intended to be converted into a functioning solar cell for a hybrid-CPV/PV system. The solar cells for this approach are manufactured by the Naval Research Lab and their dimension is 170 µm in side.
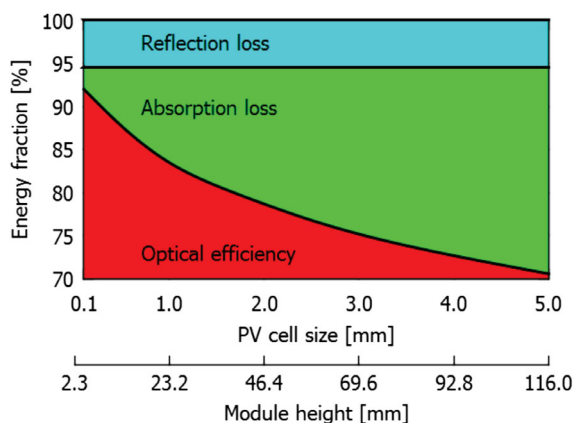
Figure 13. Calculated losses for over molded silicone encapsulation optics depending on a cell size for 200X concentration. Reproduced with permission.[111] Copyright 2013, IEEE.

cells, achieving a concentration ratio of 36X.[107] In a second iteration, two-stage optics consisting of injection molded PC lens arrays with a silicone filler between the optics stages.[108] This second version offered a concentration of 100X. A third design includes etched silicon cavities as a SOE and a POE manufactured by precision glass molding (PGM) with a concentration exceeding 500X. Designs with >1000X concentration have also been discussed.[109,110] The idea behind the incorporation of the etched silicon V-grooves is to serve not only as a high-quality nonimaging reflective stage to effectively increase CAP but also to collect diffuse light since the Si wafer can be made into a functional solar cell, leading to a hybrid micro-CPV/silicon PV approach[109] (**Figure 12**).

3.4.2. Single-Stage Optics Coupled to the Solar Cells

Micro-scale optics can benefit from the short optical paths. Absorption losses are significantly reduced, how this affects the performance is shown in **Figure 13**. Single-stage optics benefit

when enclosing the cells to the optic, this provides a high CAP (concentration acceptance product). A good example is the silicone overmolded optics used for encapsulation of LEDs discussed before.[111] The single-stage overmolded optics are only a few millimetres in size but reach concentrations of 200X with optical efficiencies exceeding 90% for cells under 400 μm in width.

The micro-CPV architecture developed by Sharp uses this approach with aspheric PMMA lenses with an aperture of 6-10 mm in width and back-contact submillimeter solar cells. They reported a concentration ratio over 300X and on-sun efficiency of 34.7%.[69]

3.4.3. TIR-Optics

Using total internal reflection (TIR) and a curved/aspheric entrance aperture, optical losses can be minimized. TIR occurs when a ray of light from a high refractive index medium reaches an interface with a medium with lower refractive index (typically air $n = 1$) at an angle below the critical angle. This ray reflects without any losses at this interface, in **Figure 14**A an optic designed for this purpose is shown and TIR is diagrammed. Such micro-CPV optical architectures support high optical transmission, since there is only one optical interface causing Fresnel reflection losses, TIR losses are negligible in theory, and adoption of highly transparent plastics such as optical-grade PMMA coupled with the short optical paths suppress bulk absorption. As an example, TIR optic designs with an acceptance angle of ±1° at 1000X and optical efficiencies over 80% have been proposed in ref. [112], this can be seen in Figure 14B. Drawbacks of TIR optics include manufacturability, shape conformity, and surface quality. Excimer laser ablation has been proposed for TIR optic fabrication,[113] although the manufacturing method is very expensive.

One of the first TIR optics applicable in micro-CPV was developed by the company Isofoton. Their optic is extremely compact, containing a TIR and an aspheric element to concentrate light onto a SOE. These optics were manufactured as a single-piece
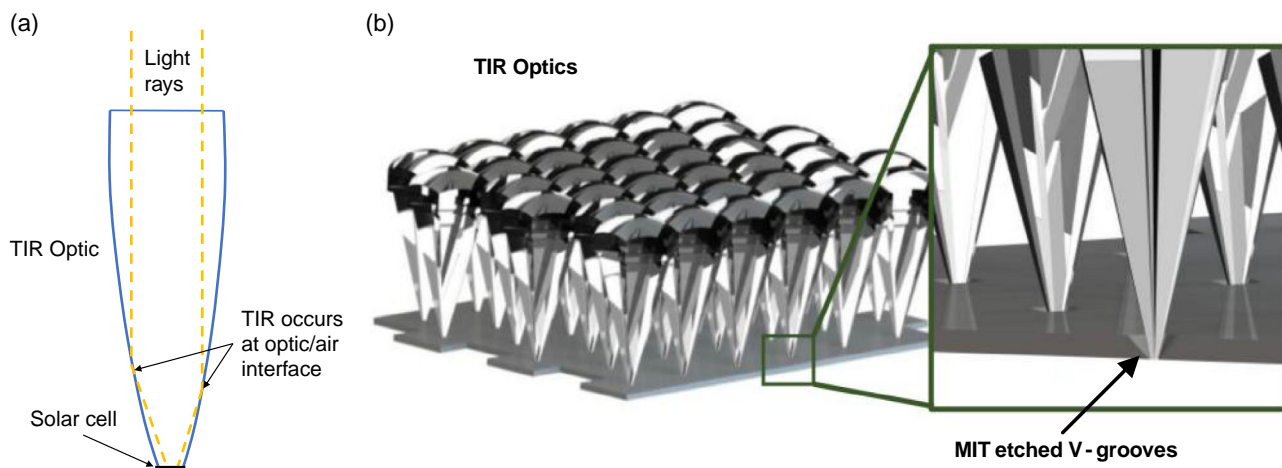
Figure 14. a) Total internal reflection (TIR) optic schematic, TIR occurs at on low incident angles when the refractive index of the medium (optic $n \approx 1.5$) is higher than the surrounding medium (air $n = 1$). b) The proposed TIR optic using MIT developed etched V-grooves in silicon. This approach showed a modeled performance of 1000X with optical efficiencies over 80%. Reproduced with permission.[112] Copyright 2019, IEEE.

PMMA component, featuring a concentration ratio of 250X and an acceptance of 2.6°.[114]

Another example of TIR optics is a 7.6X linear micro-concentrator molded with silicone, which has been described in ref. [115].

3.4.4. Waveguides

Optical waveguides operate by trapping light via multiple TIRs in a transparent medium. This approach has already been commercially used in CPV, for instance in Morgan Solars' Sun Simba panel which incorporates a light-deflecting layer coupled to a waveguide to funnel light onto the solar cell with a concentration factor of 1000X.[116] The optical parts are manufactured by PMMA injection molding, yielding a highly compact module.

Another approach uses aspheric lenses to redirect light onto a waveguide slab. The light is then channeled to the waveguide end facets where high-efficiency solar cells are placed. A planar optic reaching 300X and an optical efficiency of 82% were proposed based on this idea.[117] Waveguide films manufactured using roll-to-roll UV-NIL have been demonstrated with a concentration ratio of 4X.[118] Waveguide-integrated SOEs have also been implemented with an optical efficiency of ≈67.5%,[119] and two examples can be seen in **Figure 15**.

Optical designs based on gradient-index (GRIN) optics have been proposed to enhance waveguide coupling efficiencies at large angles.[120] A linear design was formulated with an optical

efficiency of over 95% at a moderate one-axis concentration factor of 27X.

3.4.5. Wafer Integrated

Wafer-integrated optics are directly manufactured on a Si wafer. These are a variety of proposals such as the wafer-level SOEs based on etched inverted pyramid cavities (V-grooves) seen in Figure 12 and further described in ref. [109]. Microlens array (MLA) mounted onto a solar cell using quartz etching processes[121] and micro-lens manufacturing by lithography on a substrate with CIGS solar cells[74] are other approaches that classify as wafer-integrated optics.

3.4.6. Spectral Splitting

Micro-scale solar cells further enable compact spectral splitting optics capable of spatially dividing the solar spectrum and focus the light on laterally arranged multijunction solar cells, potentially allowing optimal spectral matching. In such an approach, subcells can then be individually optimized without the constraints encountered in monolithic multijunction devices (e.g., photocurrent matching). The solar cells are grown on different substrates and then laterally arranged using transfer printing. This approach was discussed in the Section 3.1 for micro CPV. Micro solar cells are shown in Figure 8B, and an optical efficiency of 80% was experimentally validated in refs. [87,88].
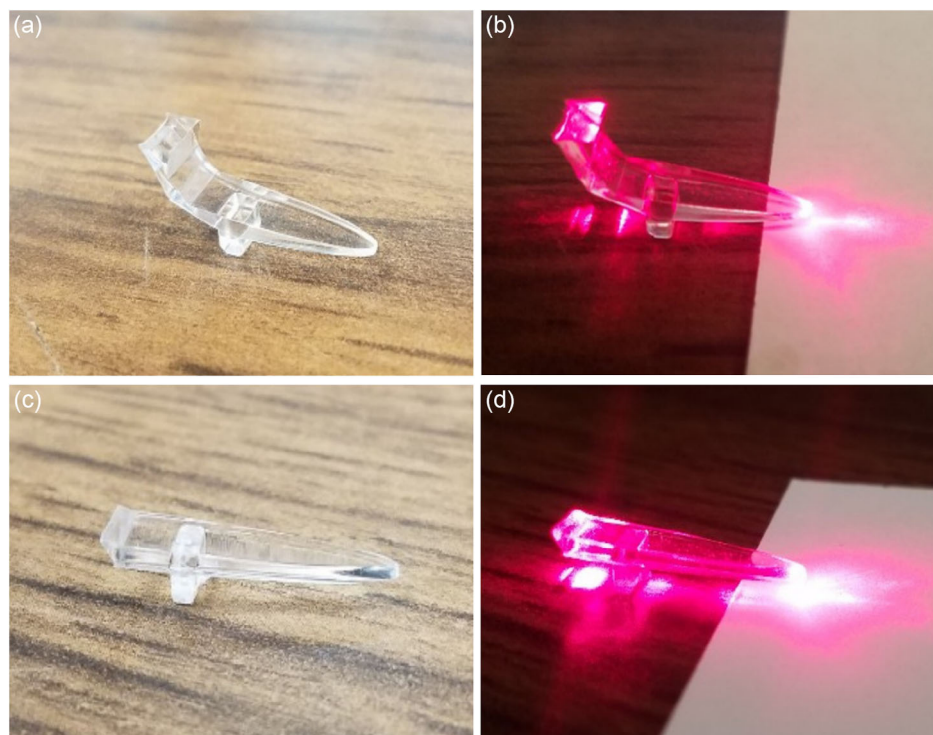
Figure 15. Waveguides manufactured using the molding of optical silicone or PMMA for micro-CPV reaching an experimental optical efficiency of 67.5%. a,c) just concentrating. In (b) and (d) the waveguides are shown under illumination onto the input surface. Reproduced with permission.[119] Copyright 2019, Optica, Formerly OSA.

ADVANCED
SCIENCE NEWS
www.advancedsciencenews.com

Solar
RRL
www.solar-rrl.com

3.4.7. Reflective

Nonimaging reflective optics have potentially higher concentrator acceptance product (CAP) since they do not suffer from chromatic aberration, although their manufacturing at micro-scale is challenging. Reflective optics also claim superior compactness and light weight, which motivated micro-CPV modules targeting space applications. A design by the Pennsylvania State University in collaboration with NRL boasts a wide acceptance angle of 9.5° optic, a concentration ratio of 18.4X, and an experimental optical efficiency of over 70%.[122] Further improved designs using glass lenses reach an optical efficiency of ≈90%.[123]

3.5. Fabrication of Large-Area Optical Arrays for Micro-CPV

Large-area micro-optics manufacturing has been a standing technical challenge. In this section, manufacturing methods applicable to micro-CPV optics will be reviewed: 1) silicone casting: a standard process for manufacturing silicone lenses on glass substrates in the CPV industry.[124] Flexible or rigid molds are used to structure the liquid silicone, which is poured onto a primed glass substrate. Then the sandwich is cured at low temperatures and later demolded and 2) hot embossing: can use rigid or flexible molds. Even molds on a roller can be used for roller-HE. The polymer is heated beyond the glassification temperature and structured with the mold. This can be used for PMMA lenses or elastomer on glass (EoG), which need an additional degasification step;[125] 3) compression-/injection-/overmolding is used for solid plastic/silicone lenses, limited in size. Overmolding is a subcategory of injection molding, adding structured material to existing parts.[42] The material is structured by injecting in viscose form (melted) into a cavity mold and then cooled before being released; 4) compression-/precision glass molding (PGM): the material with a similar shape as the final part is heated beyond the glassification temperature. A metallic plate and stamp are compressed with the viscose material in between for structuring the part. Used for aspheric glass or PMMA lens arrays or single Fresnel lenses;[126,127] 5) Roller UV-E: UV-curable resins are structured by a roller mold and progressively cured. Roll-to-roll or roll-to-plate can be used. For thin Fresnel lenses or very small bulk aspheres with depths under 100 μm;[128] 6) additive manufacturing: nano 3D-printing for aspheric or Fresnel lenses has been attempted.[129] Nanometric drops of UV-curable materials are printed by UV curing; and 7) excimer laser ablation: very localized heat is used to remove material. This is used for the structuring of deep small structures like cones for optics which use TIR (DTIRCs).[113]

Except additive manufacturing, all other processes require a mold for replication of the optics. **Figure 16** contrasts different mold manufacturing methods collected in ref. [56]. The technologies, which are most promising for micro-CPV optics, include: 1) ultraprecision machining (UPM); a) diamond turning: a fixed single diamond tip is used to cut structures into a part by turning the part on a spindle. Standard process for symmetrical structures, surface roughness (Ra) of <5 nm.[130] Used for single lens masters, not suitable for arrays; b) diamond milling: a diamond tool is turned to cut structures into a fixed part. For unsymmetrical (free-form) structures, Ra < 10 nm.[131] Can be used for lens
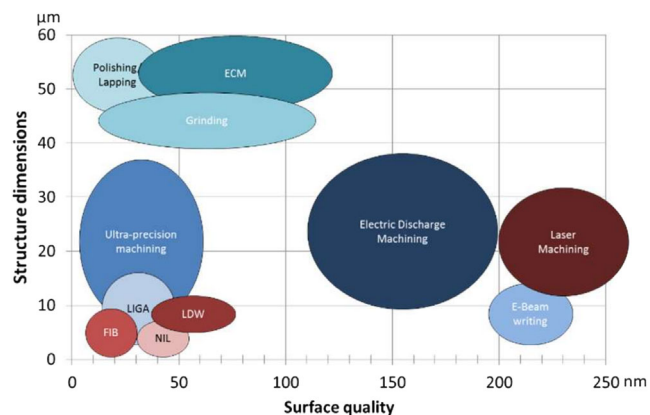
Figure 16. Mold machining technologies for optics gauged by feature size and surface quality. While not all methods listed are applicable to micro-CPV, those relevant are discussed in the text. Reproduced with permission.[56] Copyright 2019, MDPI.

array masters; c) fly cutting: the rotation of diamond blade is used to intermittently structure a fixed part. Complex microstructures are obtained by moving the blade during the cut, Ra < 10 nm.[132] Used for Fresnel structures; 2) electric discharge machining (EDM): a thin wire discharges electrically to remove great material quantities. Deep structures are possible, Ra < 0.1 μm.[133] Can be used for cone like shapes such as TIR optics (e.g., DTIRCs).

Examples of other mold manufacturing methods suited for miniature lenses or secondary optical stages include: 1) Litographie, Galvanik, and Abformung (LIGA) or X-ray lithography: PMMA is exposed to X-ray radiation then developed with chemical solvents. The cavities are filled by electroplating and the residual PMMA dissolved. Gives the possibility to structure high aspect ratios with a Ra < 10 nm,[134] 2) laser direct writing (LDW): structuring of photoresist by laser which can then be metallized and electroplated/formed, achievable Ra < 25 nm;[135] 3) electron-beam lithography and writing: photoresist structuring with low-throughput albeit with deep submicron resolution and excellent a surface finish. Ra depends on depth, Ra 2–10 nm can be achieved;[136] 4) nanoimprint lithography (NIL): limited structural flexibility as it is based on lithography with photoresists and then etching of silicon. Ra depends on process and mold materials, usually Ra < 10 nm;[137] 5) ion-beam lithography: LDW but applicable to all materials but as a much slower process, Ra < 1 nm;[138] 6) laser machining: laser ablation but can structure metal. A versatile structuring approach though suffering from low surface quality with Ra < 0.2 μm[139]

The model fabrication process may also involve a post-machining polishing/lapping step to attain very low Ra < 1 nm.[140]

For large-area optical arrays, the machined mold insert is usually not the final piece used for the molding process due to size limitations and cost of the UPM process. Electroforming is commonly used to replicate the machined surfaces and the replicas are welded together to form a large master mold. These master molds can either be directly used for optics fabrication or copied again using a polymer to obtain a soft mold. Another approach is to use multiple plastic molding steps for

making a large mold. For example, compression molding can be used for manufacturing single lenses, which are then assembled, metallized, and copied with electroforming resulting in a large-area mold.

3.5.1. Silicone Casting

In conventional CPV, the technique is commonly employed for thin silicone on glass (SoG) lens fabrication. Provided that the lens thickness does not exceed a few millimeters.[141] Mold inserts for silicone on glass lenses are machined using UPM and then copied and assembled into large area molds as described in the earlier section. Either hard nickel or soft molds made of polyurethane are used for the casting of the final lenses. Molding of the actual lens takes place by curing silicone on a glass substrate in ref. [8, p. 229]. Curing usually takes place at a temperature of ≈45 °C for 4–10 h. This temperature is chosen as it is the operating temperature of the lenses, this is done to avoid losses caused by thermal expansion.

Both bulk aspheric and Fresnel lenses can be used for micro-CPV.[141] Even for small lenses of only a few square centimeters in area, the volumetric absorption loss and lens deformation caused by thermal expansion still need to be considered. These effects were studied in ref. [141] on 200X and 500X Fresnel and bulk aspheric SoG lenses. The authors showed that the optical efficiency loss is only 1.3 percentage points lower for bulk lenses and losses caused by thermal expansion are equal between Fresnel and bulk lenses when choosing the appropriate manufacturing temperatures.

3.5.2. Hot Embossing (HE)

The processes and materials involved in HE mold manufacturing are similar to those used for SoG. PMMA and PC are the most commonly used materials for hot embossing of CPV optics in ref. [8, p. 229]. HE is appealing for its capacity of structuring large areas in comparison to, e.g., injection molding. The manufacturing cost is lower for HE as no further assembly steps are needed. Roll-to-plate HE is also a promising solution for high-throughput fabrication of micro-CPV optics.

Elastomer on glass (EoG) lenses can be manufactured by HE using a standard PV-module laminator. A vacuum must be pulled for the degasification of the solar encapsulant. These lenses use solar encapsulants such as EVA (ethyl-vinyl-acetate) or TPEs (thermoplastic elastomers), which are advantageous over silicone in terms of price and thermal properties. First prototypes have reached optical efficiencies close to SoG lenses.[125]

3.5.3. Injection/Compression Molding

Injection molding provides high throughput and excellent replication capabilities: very high aspect ratios, surface quality on par with the mold, shape tolerance of 20 μm, and edge-rounding down to 1 μm have been validated in ref. [142, p. 147]. Best results are achieved with a combination of injection-compression molding, where the mold is separated at first to guarantee proper filling of the cavities before compression to form the final geometry in ref. [142, p. 148]. This technology also allows larger parts to be molded in ref. [143, p. 47]. The main drawback of injection molding is the limited part size constrained by the injectable material volume that the feeding system can supply (usually around one liter). Injection molding offers lower cost than hot embossing when manufacturing single lenses or small optical arrays,[144] but added assembly costs make injection molding economically unfavorable for large-area optical arrays. Compression molding can circumvent this size limitation in ref. [143, p. 46], molding larger optical arrays and reduce assembly costs. Compression molding uses mold designs without feeding channels and hence of lower cost. Larger parts can be compressed, although the method is only applicable to structures with a small aspect ratio. The molding temperatures are lower in comparison to injection molding, which reduces stress, mechanical deformation, and birefringence (photoelastic refractive-index variation due to internal material stresses) in ref. [142, p. 132].

The molds for plastic molding are customarily manufactured by UPM, but other machining mechanisms are also used as showcased in ref. [145].

A specific injection molding technique is over molding, a process widely used in chip on board (COB) packaging for LEDs.[100] In this low-temperature and pressure molding process, a material is molded onto another part. The most common materials are high refractive index silicones, or other materials, such as thermoplastic elastomers, can also be used. For micro-CPV, this could be an attractive technology for integrating SOE on cells or even for the manufacturing of single-staged micro-optics. Specific processes have been developed for over molding of optics, such as low-pressure molding which is between conventional injection molding and traditional casting. This method can be used for bulk silicone optics,[144] e.g., Insolights' first lenses before switching to PMMA injection molding.[42] Another alternative is silicone transfer molding,[146] a technology between injection and compression, achieving larger parts than injection molding but affording surface tolerances similar to compression molding.

3.5.4. Compression-Modling/Precision Glass Molding (PGM)

Compression molding of glass lenses is more suitable for bulk aspheric lenses designs than Fresnel lenses due to manufacturing limitations of the PGM process. It should be noted though that Fresnel lenses have also been prototyped.[147] A collaboration between Holophane S.A.S. and the IES-UPM resulted in prototype aspheric bulk lens arrays have demonstrated experimental optical efficiencies over 80% at a concentration of ≈180X, and performance improvements are anticipated with further prototype iterations.[126]

Standard PGM, as depicted in **Figure 17**, uses compression molding with molds usually manufactured by diamond milling. A limitation is that only one side of the glass sheet can be structured, the other side must be polished to remove surface contaminations during the process. Surface roughness of 10 nm and shape tolerances of 25 μm can be achieved in ref. [142, p. 197]. Edge rounding can be brought down to 1–10 μm for small parts such as single Fresnel lenses.[147]
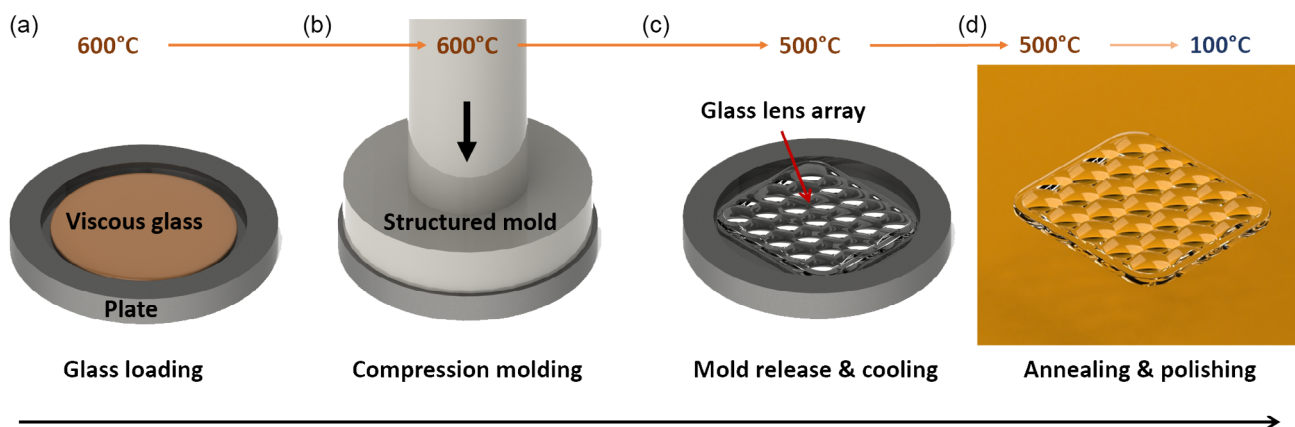
Figure 17. The precision glass molding process as described from the company Holophane S.A.S. a) The moldable glass is loaded onto a plate and heated beyond the glassification temperature. b) A compression molding process is used to structure the glass, c) a short cooling phase allows for rapid demolding. d) The last step is annealing, polishing, and cutting the excess glass. Reproduced with permission.[126] Copyright 2022, Elsevier.

Unlike plastics, birefringence is usually not an issue in glass in ref. [142, p. 196], and thus losses caused by refractive index non-uniformity are very low. Due to the nature of the compression molding process, PGM is best suited for fabricating structures with relatively low aspect ratios. Nonetheless, the high material quality and the low manufacturing cost qualify the PGM technology as a viable solution for processing aspheric bulk lens arrays for micro-CPV.

Roller molding on glass is another technology, which is currently being developed for reducing the cost of precision structured glass.[148]
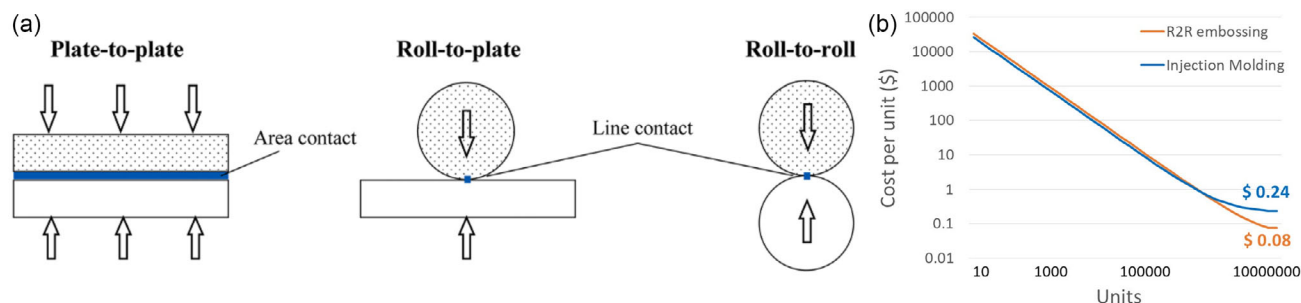
3.5.5. Roll-To-Roll, Roll-To-Plate, and Plate-To-plate

Depending on the initial and final substrates, the approach encompasses three variants: plate-to-plate (P2P), roll-to-plate (R2P), and roll-to-roll (R2R) (**Figure 18**A). P2P is usually first matured before being transitioned to R2P and R2R when applicable. The transition is motivated by massive throughput enhancement and cost reduction facilitated by roll-based processes compared to other embossing or injection technologies at large volumes[55] (Figure 18B). Micro-CPV optics must eventually be assembled onto a plate, so R2R would require an

additional step (compared to R2P or P2P) of laminating the optic film on a plate.[128]

R2R, R2P, and P2P optics manufacturing can utilize either thermal or ultraviolet nano-imprint lithography (T-NIL and UV-NIL), both of which are proven low-cost and high-throughput processes for replicating micro- and nano-scale patterns including micro-optics.[149] For example, small Fresnel structures can be manufactured with high-throughput using roll-to-roll/plate hot-embossing (T-NIL) or UV-NIL, even though Fresnel designs of primary lenses are not strictly necessary for micro-CPV given the deeply downscaled lens depth. In both T-NIL and UV-NIL, imprinted resins are swiftly cured on films or rigid substrates.[55] The best results currently achieved by roll-to-roll UV-embossing are Fresnel lenses with a concentration of over 100X[128] (**Figure 19**).

The molds for roller embossing are either very thin nickel electroforms mounted on the roller (in T-NIL) or silicone copies of the machined structures (UV-NIL).[149] Silicone is chosen for UV-NIL because of its low cost and UV transparency.[150] Recent studies have explored using UV-curable resins as a mold material for roller T-NIL of small structures with a depth of 0.4 μm.[151] Recently, five-axis computer numerical control (CNC) machining was also harnessed to directly machine Fresnel structures on a roller mold.[55,152]

Figure 18. a) Showing the technological evolution of massive throughput optical molding, roll-to-plate, and roll-to-roll are suitable for Fresnel lenses. Reproduced with permission.[149] Copyright 2014, Springer. The first being better for micro-CPV as no additional laminating step would be needed. b) Compares costs for roll-to-roll embossing and injection molding for LED optics. Reproduced with permission.[55] Copyright 2019, Springer.
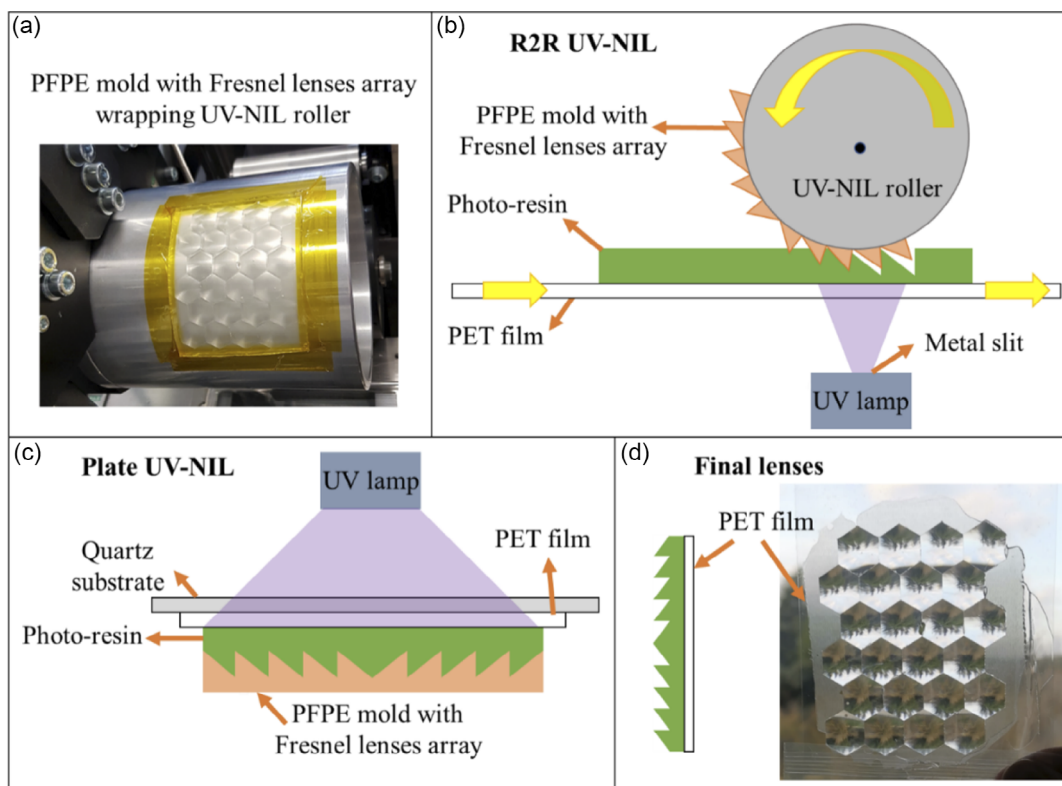
Figure 19. Micro-CPV optics manufactured by roll-to-roll UV-NIL using b) a flexible mold and c) Plate UV-NIL. a) The flexible mold is seen on the roll and d) shows a final lens on a flexible polymer substrate. Reproduced with permission.[128] Copyright 2021, Optica.

High-quality CPV lenses have been demonstrated with UV-NIL in R2P and R2R by the Imdea Nanoscience in collaboration with the IES-UPM using optical resins from the company Film Optics Ltd and a R2R machine from the company PTMTEC.[128] The groove depth of the UV-NIL processed Fresnel structure is limited to 50–100 μm depending on the resin used and how the mold is manufactured. UV-NIL has also been used to engrave antireflective coatings (ARC).[153] Both the flat side and the Fresnel surface of the lens can be imprinted with ARC structures.[154]

T-NIL (hot embossing) is often preferred over UV-NIL due to the high price of UV-curable resins ($30 kg^{-1} according to)[55] and their unproven long-term stability under outdoor conditions. T-NIL has yielded good results for P2P and R2P micro-lens fabrication.[155] R2R T-NIL is, however, challenging since the film tension needed to structure the surface tends to deform or break the softened polymer (PMMA) at elevated temperatures, better results were obtained on PVC or PET films.[156]

3.5.6. Additive Manufacturing

Micro- and nano-scale 3D printing is a versatile emerging technology for complex 3D structures with low surface roughness of the order of nanometers.[157] The readers are referred to a review on 3D-printed micro-optics.[158] Luximprint is a company at the forefront of the technology.[159] Micro-lenses have been demonstrated with good performance, although Fresnel

lenses remain a fabrication challenge for 3D printing since the dimensional accuracy and resolution of the printing process must be further improved. The printed polymer materials are highly transparent in their as-printed state.[129] However, discoloration may occur when they are exposed to outdoor conditions over time, and long-term durability remains a concern. That said, this technology presents a viable solution for printing low-cost optical masters for mold replication. Its unique capability of creating complex 3D structures also enables fabrication of advanced mold structures not be possible using conventional machining.

3.6. Synergies with Other Industries

The component size downscaling in micro-CPV paves a path with wide opportunities toward adoption of high-throughput manufacturing processes matured in other industries. Such synergies across different industries are a key strength of micro-CPV for its continued development and innovations. This paper has reviewed many of these technologies that can be potentially applied for high-volume manufacturing of micro-CPV. In the following **Table 6**, we summarize the examples.

One of the highest contributors is the development of micro-LED screens within the display industry.[92] They face a similar technological challenge as micro-CPV; a large number of tiny dies which must be positioned and interconnected with micron-level precision.[45,75] Transfer printing is one of the technologies that has already been used and proven to work for the

Table 6. Examples of synergies with other industries for micro-CPV.

Technology	Description	Industry	Reference
Micro-transfer printing	Solar cell placement with high throughput. Applied in micro-CPV	Display/lighting industry: micro-LEDs for screens and illumination. Companies: X-Celeprint, Microprince	[43,84]
Fluid self-assembly	Automatic placement and adhesion of dies on a flexible or rigid substrate. The process has been tested for micro-CPV	Display/lighting industry: micro-LEDs for screens and illumination. Company: eLux	[79]
Printing of interconnects	Printing of the electric circuit for interconnection of dies on a large rigid substrate. Utilized in micro-CPV	Display/lighting industry: micro-LEDs for screens and illumination	[44,54]
Chip-on-board (COB) packaging	Avoid wire bonding dies on a large area as the dies are prepared on small boards. These boards are then reflow soldered on the final large substrate. Applied in micro-CPV	Display/lighting industry: micro-LEDs for screens and illumination	[44,105]
Micro-optics	Miniature optics can be integrated on COB. Utilized in micro-CPV as SOE and POE	Display/lighting industry: micro-LEDs for screens and illumination	[22,44]
Roll-to-roll/plate optics	Both roll-to-roll and to-plate can be used for high-throughput manufacturing of Fresnel lenses or micro lenses. The process has been tested for CPV lenses	Lighting/automotive industry: optics. Company: Film Optics	[55]
Precision glass molding	Most suitable for fabricating non-Fresnel bulk-lenses for micro-CPV. The process has been used for micro-CPV prototypes	Lighting/automotive industry: optics. Companies: Holophane, Isuzu Glass	[126,162]
Printing and interconnection of devices on large areas	Applied in micro-CPV for the interconnection of solar cells	Telecommunications industry: RFID	[54]
Printing of interconnects on flexible substrates	Flexible micro-CPV modules for car-PV, mobile chargers, etc.	Telecommunications industry: RFID	[163]
Hot-embossing of plastics	Potential uses for micro-CPV optics	Medical industry: lab-on-chip devices	[125]
Very precise packaging technologies	COI (chip-on-interposer) and large-area assembly	Photonics industry	[44]
Waveguides	Light-guiding optics such as the examples given in Table 1	Photonics industry	[37,116]

placement of dies.[43,99] FSA is an additional die-placement technology developed for micro-LEDs,[78] which has been validated for micro solar cells.[79] The cross-pollination from the micro-LED industry has already facilitated the development of various micro-CPV prototypes.[44,63,79] It will further contribute to reducing the cost in assembly and manufacturing of components of micro-CPV modules to expedite commercial deployment of the technology. The ability to leverage existing industrial infrastructure hands micro-CPV a critical advantage over the classical CPV technology, as the latter relies on considerable hand labor or dedicated tools lacking economy of scale.

4. Advanced Architectures Enabled by Micro-CPV

The market potential for CPV is fundamentally limited by the need of high-precision two-axis tracking structures and the inability of concentrator optics to capture diffuse radiation. However, micro-CPV technology is particularly suited for the adoption of novel module architectures enabling static module mounting (via integrated planar micro-tracking) and utilizing both direct and diffuse fractions of the incident irradiance (via hybrid CPV/silicon PV architectures).
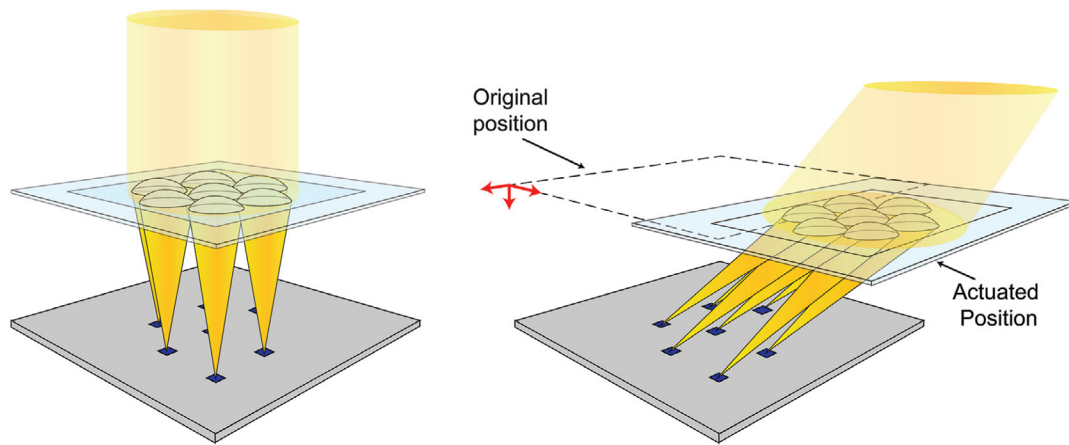
4.1. Integrated Tracking for Micro-CPV

Micro-scale optics enables the integration of mechanical tracking systems with minimal movement inside the PV modules so that the modules can be installed in a fixed structure without involving external solar tracking systems. Such internal tracking systems require a minimum of two tunable optical surfaces to focus on- and off-axis ray sets.[35] Insolight proposed an optical design based on a double convex aspheric lens and an over molded SOE, achieving a concentration ratio of $\approx$200X and a tracking range exceeding $\pm$50°,[34,44] (**Figure 20**). These tracking ranges are sufficient for a functioning tracking during the duration of the day. This concept unlocks the residential and agrivoltaic PV markets, applications where efficiency is valuable. Insolight achieved exceptionally large acceptance with a biconvex aspheric lens array.[52,55] Other optical architectures have also been proposed.[160]

Catadioptric designs combining aspheric refractive and reflective surfaces have also been proposed, see **Figure 21**. Simulation results indicate optical efficiencies of over 90% for AOIs (angles of incidence) between 0 and 60° and concentrations between 500 and 1700X.[161] Price et al.[41] developed a catadioptric optical system, which focuses sunlight onto a middle plane where the micro-CPV cells are placed. The cells are sandwiched between a pair of glasses bonded with optical adhesive, and the sheet slides between the top and bottom lenses to align the sun focal spot at different solar incidence angles with the cells.

A radically different approach couples the incident light into a planar waveguide. The scheme is compatible with both external and internal tracking, in this latter case by lateral translation between the optics and the planar waveguide. The efficiency is limited by high absorption of the waveguide material, yet this is a surmountable challenge in the future.[37]

Figure 20. Insolight integrated tracking micro-CPV using a biconvex molded optic with very high acceptance. The solar cell plane is repositioned during the day with actuators into the focal point of the concentrator lenses. These optics have shown high performance with an on-axis optical efficiency of 82% and a tracking scope of 58° where 50% of the on-axis efficiency is lost. Reproduced with permission.[173] Copyright 2017, John Wiley & Sons, Inc.
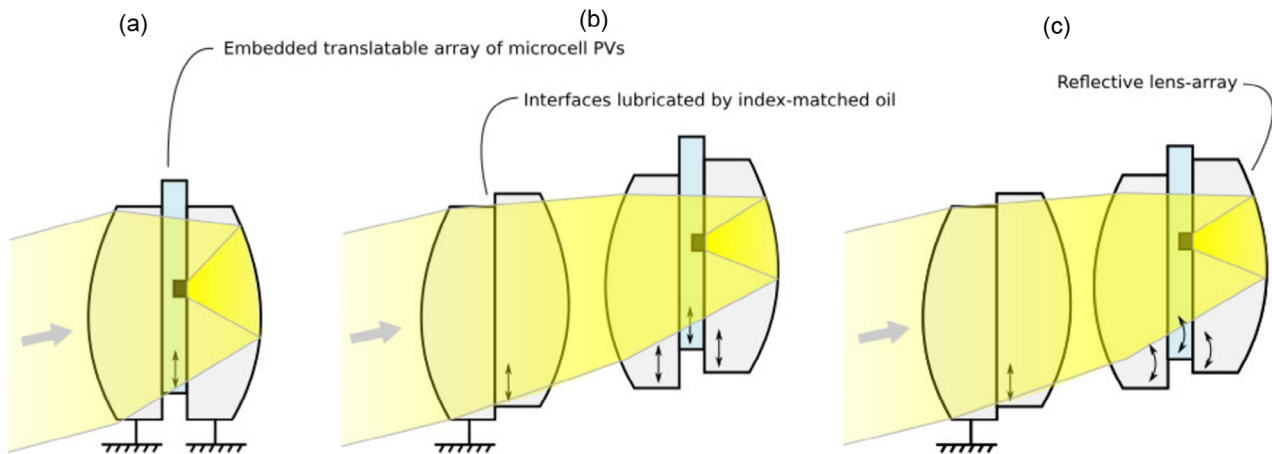
Figure 21. a) Catadioptric optic approach for micro-CPV as used by Glint photonics. Reproduced with permission.[41] Copyright 2017, Springer Nature. Adding multiple stages (b) and different translation types (c) increases the tracking range, concentration, and optical efficiency. Reproduced with permission.[161] Copyright 2019, SPIE.

To summarize the current prototypes, in **Table 7**, we present an extension of Table 1, in which we defined certain parameters to facilitate comparison between the technologies: 1) integrated tracking span (T_{Span}): the incidence angle at which the optical efficiency drops to 90% of maximum efficiency. This is equivalent to the optical acceptance angle in the presence of tracking, resulting in expanded acceptance angles compared to static systems. 2) Integrated tracking scope (T_{Scope}): the incidence angle at which the optical efficiency drops to 50% of maximum efficiency. This parameter should be as close as possible to 60°, which corresponds to an ideal cosine response. 3) Integrated tracking range (T_{Range}): this parameter determines the angle at which the tracking system is mechanically limited. It should be over 60° to cover the sun trajectory in most locations. 4) Hybrid DNI/diffuse capture: methods that include secondary low-cost silicon PV cells to capture not only the diffuse irradiance but also DNI spillage.

The latter refers to light deviated from designed optical path due to scattering and/or misalignment of the optical system and not focused onto the primary micro-CPV cells, which can be harvested by the secondary silicon PV cells. A hybrid system recovers lost rays when tracking errors occur or when the tracking range is insufficient to cover the whole trajectory of the sun. 5) Concentration tracking span product (CTP). For comparison between tracked-CPV technologies, we define a specific figure of merit, similarly to the CAP for conventional CPV. CAP is limited by the étendue limit given by the acceptance of optic when the system is mechanically fixed, but a different figure is needed to account for the angular performance of internal tracking. We hereby define CTP given by Equation (2). For example, transmissive micro-tracked systems have shown significantly enhanced CTPs between 1 and 9 (comparing to CAPs of up to 0.5). A CTP of ≈28 was achieved using a catadioptric (lens + back reflector) design.[41]

Table 7. Overview of integrated tracking micro-CPV prototypes. The parameters are collected from the references shown in the last column.

| X [suns]	η [%]	On-axis opt. eff. [%]	Int. Tracking Span @90%EffOptical [°]	CTP	Int. Tracking scope @50%EffOptical [°]	Int. Tracking range [°]	Hybrid capable	Cell Size [μm]	Description	Reference
660	30	93	70	24.14	80	80	No	650	3J micro cells on a sliding glass encapsulated with liquid optical grade oils in a Cassegrain optic out of a glass top and bottom. (Glint Photonics)	[41]
180	29	82	44	9.32	58	70	Yes	1000	3J micro cells on a 3-axis moving plane, overmolded silicone SOE and a biconvex PMMA POE with high acceptance (55°). These modules can be translucent or hybrid. (Insolight)	[44]
300		81	–	–	–	23.5 (1D)	Yes	–	POE combined with a slab waveguide, concept uses combinations of exterior (2-axis) and integrated (lateral) tracking. (UC San Diego)	[117,183]
127	30	82	45	7.97	65	70	Yes	1000	3J micro cells on a three-axis moving plane using a ball guide which accurately positions on the Petzval field projected by the single-stage PMMA bi-convex optic. (Nagaoka U.)	[34]
330	26	–	–	–	–	–	Yes	550	3J micro cells with a tilt and roll integrated tracking using biconvex PMMA lenses. This system is also hybrid, both parts the Si-PV and IIIV show efficiencies of 26% at equal DNI and GNI Irradiance. Losses with this concept is caused by shading. (Panasonic Boston Lab.)	[184,185]
8.6	–	80	30	1.47	40	40	Yes	375	2J micro cells with aspheric silicone microcells. The lateral displacement tracking uses actuator and a 3D guide rail for positioning in the z-axis. (GIST)	[36]
128	–	70	10	1.96	20	30	Yes		Not yet tested with solar cells, an aspheric injection molded lens concentrating onto a waveguide. The lateral displacement tracking using a worm-driven motor for very precise positioning. (UC San Diego)	[37]
250	–	79	23	6.18	–	–	Yes		Not yet tested with solar cells. Commercially available acrylic aspheric lens with a PMMA waveguide. Tracking with a two-axis displacement of the waveguide. (Texas A&M University)	[38]
250	–	79	32	8.38	–	–	No		Si photodetector with 2 PMMA lens arrays and a waveguide. Self-tracking using phase-change materials (Parafin) by melting and coupling the light. (Texas A&M University)	[186]

$$CTP = \sqrt{X} * \sin(T_{Span}) \qquad (2)$$

Among the integrated tracking prototypes presented in Table 7. The best overall performance is attained by Price et al.[41] with a high concentration factor of 660X and a CTP of 24. The drawback is that the catadioptric optic is not compatible with integration with a hybrid system, making it unable to capture diffuse light. The Insolight module is the closest to a commercial product and has the potential for further increasing the current concentration values.[44]

4.2. Hybrid Micro-CPV/Silicon PV Architectures for Utilization of Direct and Diffuse Solar Irradiance

The hybrid micro-CPV/silicon PV concept aims at increasing the energy yield of CPV technologies by harvesting the diffuse light not utilized by CPV with a PV backplane made of crystalline silicon. This concept is being explored by various research institutes such as MIT, NRL, and Fraunhofer ISE, as well as companies including Toyota, Panasonic, and Insolight toward commercialization.[44,106,109,162–164]
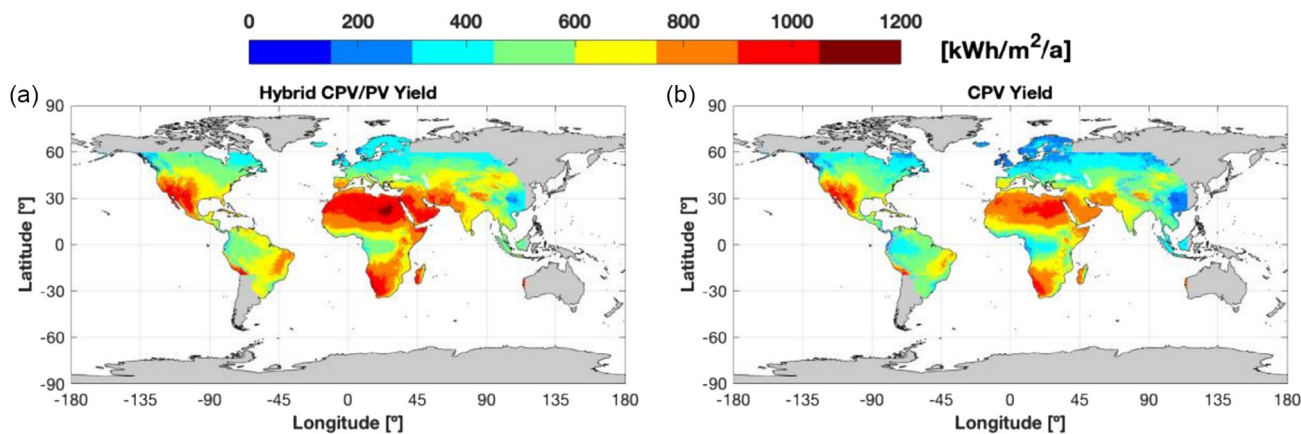
Figure 22. Yearly energy yield comparing a) hybrid CPV/PV to b) the standard CPV technology, in the publication more cases are compared. Reproduced with permission.[166] Copyright 2021, Cell Press.
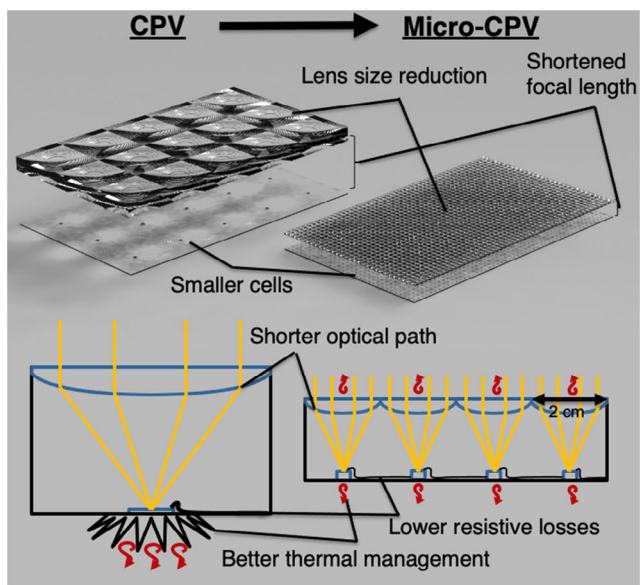
Figure 23. Illustration of the main functional benefits of micro-CPV modules compared to conventional CPV. The reduction of the solar cell size and the optical aperture result in advantages such as shorter optical paths, lower resistive losses and better thermal management. An additional benefit is more flexibility for different interconnection schemes, these can avoid power losses generated by misalignments between solar cells and optics.

The combined power production of this technology varies significantly depending on the ratio of direct normal irradiance to diffuse irradiance.[165] **Figure 22** compares the technology to conventional CPV across geographic locations around the world. The average global yearly yield advantage to CPV is 20.4%. The same authors further drew quantitative comparisons between the hybrid technology and tracked/static silicon PV.[166]

The hybrid approach must leverage low-cost, scalable manufacturing methods established in the silicon PV industry to be competitive in the market. A good example is the Insolight hybrid micro-CPV/silicon PV module. The manufacturing procedure entails encapsulating the

interconnected Si-cells between two glass planes. On top of the glass plane, the metal interconnects for the III–V cells are printed and the III–V solar cells, which have been encapsulated as a chip-on-interposer device with all backside contacts, are attached with a conductive adhesive.[44]

4.3. Reducing Cell-To-Module Power Loss Using Micro-CPV

A collection of benefits of micro-CPV modules is shown in **Figure 23**, which led to an important reduction of losses of 10% from the solar cells, with efficiencies of around 45% on an industrial scale, to final modules with efficiencies of around 35%. These losses are mainly to optical losses, thermal losses, resistive losses, and misalignment of the optic-solar cell pair. The first three of these can be improved by micro-CPV. For the latter, as mentioned previously, solutions are found by synergies with other industries. How the first three are addressed is described as follows.

These modules contain a large number of cell-optic pairs which prompts new interconnection designs[93] taking advantage of a combination of parallel and series interconnections. Such designs can reduce power losses due to defects, misalignment, optical and electrical mismatches, and/or cell power variability. This also gives the possibility to achieve an output voltage comparable to a conventional silicon PV module.

Thermal losses are lower for micro-CPV since heat dissipation is efficient given the much larger perimeter-to-area ratio afforded by the micro-PV cells. Simulations have shown that 550 μm sided solar cells mounted on a glass board (low heat dissipation) at 1000X promise temperatures below 120 °C at open-circuit voltage (V_{OC}).[167] In case cooling is necessary due to extremely high concentrations, there are options which can be applied to micro-CPV.[168]

The size reduction leads to shorter optical paths, as mentioned in Section 3.4 Advanced optical approaches for micro-CPV there are multiple ways to increase the optical efficiency. From just reducing the optical material volume to using high-quality materials and/or high optical performance optics.

Misalignment between cells and optics poses an even greater challenge in micro-CPV.[58,114] The submillimeter size leads to low mechanical tolerances (10–100 μm) so high precision manufacturing and assembly processes are mandatory, a challenge which conventional CPV faces and only exacerbates in micro-CPV. Self-alignment processes have been proposed making use of surface tension of melted solder, achieving cell positioning accuracy within ± 10 μm.[71] Another approach involves joint molding of POE and SOE so that their relaive position is defined by the mold.[169,170] Misalignment due to differential thermal expansion of dissimilar materials is another concern, and using the same material for the optical layer and cell plane reduces notably this effect.[44]

In ref. [171] an extensive study reveals micro-CPV can indeed furnish a competitive edge in curtailing the cell-to-module power loss compared to traditional CPV. The ratio between module efficiency and cell efficiency was calculated, which led to the conclusion that micro-CPV reaches a ratio of 93% while in conventional CPV the ratio is only around 75%.

5. Conclusions

Micro-CPV charts a roadmap to future low-cost, high-efficiency PVs for large-scale electricity generation. The size downscaling of micro-CPV provides benefits such as short optical path, better thermal management, lower resistive losses, low weight, and a compact module form factor similar to that of silicon PV. Additional features include internal tracking and hybrid CPV/silicon-PV, micro-CPV is well poised for space-constrained applications such as space solar, rooftop installations, agrivoltaics, vehicle-integrated PVs, large off-grid power systems, mobile chargers, among others. Nonetheless, new module architectures as well as enabling manufacturing technologies are needed to allow large-scale commercial deployment of the technology. We show that manufacturing of micro-CPV can capitalize on infrastructures and technical expertise from mainstream industries like telecommunications, lighting, automotive, medical, and photonics industries for mass production and cost scaling. Examples of directly transferable technologies include parallel assembly and interconnection of small devices and large-area scalable micro-optic fabrication. In addition, micro-CPV allows the exploration of unconventional device architectures that typically could not be adopted by classical macro-scale CPVs toward further performance enhancement.

This review scrutinizes the state of the art of the technology, covering advances on micro solar cell development, solar cell assembly solutions, functional interconnection of the micro solar cells, novel optical designs and manufacturing, the integration of hybrid micro-CPV/silicon PV, and internal tracking within a compact, flat module. Figure 1, Table 1 and 7 are meant to provide the reader with a comprehensive overview of the performance of current micro-CPV modules. Micro-CPV prototype modules with efficiencies close to 35% have already been demonstrated, and modules exemplified by those manufactured by Insolight are starting to penetrate into niche markets. It is highly anticipated that these advances will further prove the viability and lead to a lasting presence of the micro-CPV technology in the global energy market.

Conflict of Interest

The authors declare no conflict of interest.

[1] Fraunhofer ISE, *Photovoltaics Report*, Fraunhofer-Gesellschaft **2021**, https://www.ise.fraunhofer.de/content/dam/ise/en/documents/annual_reports/fraunhofer-ise-annual-report-2021-2022.pdf (accessed: June 2020).

[2] A. Goodrich, P. Hacke, Q. Wang, B. Sopori, R. Margolis, T. L. James, M. Woodhouse, *Sol. Energy Mater. Sol. Cells* **2013**, *114*, 110.

[3] S. P. Philipps, A. W. Bett, K. Horowitz, S. Kurtz, *Current Status of Concentrator Photovoltaic (CPV) Technology*, National Renewable Energy Lab.(NREL) **2015**, pp. 1–25, https://www.nrel.gov/docs/fy16osti/65130.pdf (accessed: June 2020).

[4] A. Luque, G. Sala, I. Luque-Heredia, *Prog. Photovoltaics Res. Appl.* **2006**, *14*, 413.

[5] R. M. Swanson, *Prog. Photovoltaics Res. Appl.* **2000**, *8*, 93.

[6] S. Kurtz, *Prog. Photovoltaics Res. Appl.* **2007**, *15*, 659.

[7] P. Benítez, J. C. Miñano, P. Zamora, R. Mohedano, A. Cvetkovic, M. Buljan, J. Chaves, M. Hernández, *Opt. Express* **2010**, *18*, A25.

[8] C. Algora, I. Rey-Stolle, *Handbook of Concentrator Photovoltaic Technology*, John Whiley & Sons Inc. **2016**, pp. 1–772, ISBN: 978-1-118-47296-5.

[9] M. Wiesenfarth, I. Anton, A. W. Bett, *Appl. Phys. Rev.* **2018**, *5*, 041601.

[10] J. F. Geisz, R. M. France, K. L. Schulte, M. A. Steiner, A. G. Norman, H. L. Guthrey, M. R. Young, T. Song, T. Moriarty, *Nat. Energy* **2020**, *5*, 326.

[11] M. Steiner, G. Siefer, T. Schmidt, M. Wiesenfarth, F. Dimroth, A. W. Bett, *IEEE J. Photovoltaics* **2016**, *6*, 1020.

[12] K. A. W. Horowitz, M. Woodhouse, H. Lee, G. P. Smestad, *Cpv-11* **2015**, *100001*, 100001.

[13] C. A. Gueymard, *Proc. SPIE 7046, Optical Modeling and Measurements for Solar Energy Systems II*, 70460D, San Diego, CA, September 2008, **2008**, https://doi.org/10.1117/12.795506.

[14] M. W. Haney, T. Gu, G. Agrawal, in *Photovoltaic Specialists Conf. (PVSC), 2014 IEEE 40th, no. c*, IEEE, Piscataway, NJ **2014**, pp. 2122–2126.

[15] G. Smestad, H. Ries, R. Winston, E. Yablonovitch, *Sol. Energy Mater.* **1990**, *21*, 99.

[16] N. Shatz, J. Bortz, R. Winston, *Opt. Express* **2010**, *18*, A5.

[17] R. Winston, J. C. Miñano, P. Benitez, N. Shatz, J. C. Bortz, *Nonimaging Opt.* **2005**.

[18] J. C. Miñano, P. Benítez, P. Zamora, M. Buljan, R. Mohedano, A. Santamaría, *Opt. Express* **2013**, *21*, A494.

[19] P. Gleckman, J. O'Gallagher, R. Winston, *Nature* **1989**, *339*, 198.

[20] R. Winston, *High Collection Nonimaging Optics*, Vol. *1038*, Academic Press, New York and London **1989**.

[21] T. Gu, D. Li, L. Li, B. Jared, G. Keeler, B. Miller, W. Sweatt, S. Paap, M. Saavedra, U. Das, S. Hegedus, in *Photovoltaic Specialist Conf. (PVSC), IEEE 44th*, Vol. *080004*, IEEE, Piscataway, NJ **2017**.

[22] H. Arase, A. Matsushita, A. Itou, T. Asano, N. Hayashi, D. Inoue, R. Futakuchi, K. Inoue, T. Nakagawa, M. Yamamoto, E. Fujii, *IEEE J. Photovoltaics* **2014**, *4*, 709.

[23] A. L. Lentine, G. N. Nielson, M. Okandan, J. L. Cruz-Campa, A. Tauke-Pedretti, *IEEE J. Photovoltaics* **2014**, *4*, 1593.

[24] T. Gu, D. Li, L. Li, B. Jared, G. Keeler, B. Miller, W. Sweatt, S. Paap, M. Saavedra, U. Das, S. Hegedus, in *OSA Light, Energy and the Environment*, Leipzig, Germany, November **2016**.

[25] M. W. Haney, in *Photovoltaic Specialists Conf. (PVSC), IEEE 44th*, IEEE, Piscataway, NJ **2017**.

[26] X. Sheng, C. A. Bower, S. Bonafede, J. W. Wilson, B. Fisher, M. Meitl, H. Yuen, S. Wang, L. Shen, A. R. Banks, C. J. Corcoran, *Nat. Mater.* **2014**, *13*, 593.

[27] K. T. Lee, Y. Yao, J. He, B. Fisher, X. Sheng, M. Lumb, L. Xu, M. A. Anderson, D. Scheiman, S. Han, Y. Kang, *Proc. Natl. Acad. Sci.* **2016**, *113*, E8210.

[28] A. Carlson, A. M. Bowen, Y. Huang, R. G. Nuzzo, J. A. Rogers, *Adv. Mater.* **2012**, *24*, 5284.

[29] T. Gu, G. Agrawal, A. Vessey, W. C. Sweatt, B. H. Jared, J. L. Cruz-Campa, R. Goeke, W. K. Miller, D. L. Zamora, E. Langlois, M. Okandan, in *2015 IEEE 42nd Photovoltaic Specialist Conf. (PVSC)*, IEEE, Piscataway, NJ **2015**.

[30] G. N. Nielson, M. Okandan, J. L. Cruz-Campa, A. L. Lentine, W. C. Sweatt, V. P. Gupta, J. S. Nelson, *Micro-Nanotechnol. Sens., Syst. Appl. IV* **2012**, *8373*, 837317.

[31] K. Ghosal, D. Lilly, J. Gabriel, M. Whitehead, S. Seel, B. Fisher, J. Wilson, S. Burroughs, *IEEE J. Photovoltaics* **2014**, *4*, 703.

[32] B. H. Jared, M. P. Saavedra, B. J. Anderson, R. S. Goeke, W. C. Sweatt, G. N. Nielson, M. Okandan, B. Elisberg, D. Snively, J. Duncan, T. Gu, *Opt. Express* **2014**, *22*, A521.

[33] K. A. W. Horowitz, D. W. Cunningham, J. Zahler, in *OSA Light, Energy, and the Environment*, Boulder, CO, November **2017**, p. RM3C.4.

[34] A. Ito, D. Sato, N. Yamada, *Opt. Express* **2018**, *26*, A879.

[35] F. Duerr, Y. Meuret, H. Thienpont, *Opt. Express* **2011**, *19*, A207.

[36] T. Lim, P. Kwak, K. Song, N. Kim, J. Lee, *Prog. Photovoltaics Res. Appl.* **2017**, *25*, 123.

[37] J. M. Hallas, K. A. Baker, J. H. Karp, E. J. Tremblay, J. E. Ford, *Appl. Opt.* **2012**, *51*, 6117.

[38] Y. Liu, R. Huang, C. K. Madsen, *Opt. Express* **2014**, *22*, A1567.

[39] H. Ma, L. Wu, *Appl. Opt.* **2015**, *54*, 6217.

[40] J. S. Price, X. Sheng, B. M. M, eublblok, J. A. Rogers, N. C. Giebink, *Nat. Commun.* **2015**, *6*, 6223.

[41] J. S. Price, A. J. Grede, B. Wang, M. V. Lipski, B. Fisher, K. T. Lee, J. He, G. S. Brulo, X. Ma, S. Burroughs, C. D. Rahn, *Nat. Energy* **2017**, *2*, 17113.

[42] G. Nardin, C. Domínguez, Á.F. Aguilar, L. Anglade, M. Duchemin, D. Schuppisser, F. Gerlich, M. Ackermann, L. Coulot, B. Cuénod, D. Petri, *Prog. Photovoltaics Res. Appl.* **2020**, *29*, 819.

[43] S. Burroughs, R. Conner, B. Furman, E. Menard, A. Gray, M. Meitl, S. Bonafede, D. Kneeburg, K. Ghosal, R. Bukovnik, W. Wagner, *AIP Conf. Proc.* **2010**, *1277*, 163.

[44] G. Nardin, *Prog. Photovoltaics* **2020**, *29*, 3.

[45] T. Wu, C. W. Sher, Y. Lin, C. F. Lee, S. Liang, Y. Lu, S. W. Huang Chen, W. Guo, H. C. Kuo, Z. Chen, *Appl. Sci.* **2018**, *8*, 1557.

[46] A. Paranjpe, J. Montgomery, S. M. Lee, C. Morath, *SID Symp. Dig. Tech. Pap.* **2018**, *49*, 597.

[47] P. Espinet-González, I. Rey-Stolle, M. Ochoa, C. Algora, I. García, E. Barrigón, *Prog. Photovoltaics Res. Appl.* **2015**, *23*, 874.

[48] P. Albert, A. Jaouad, M. Darnon, A. Volatier, in *Int. Symp. on Reliability of Optoelectronics System*, Toulouse, France, November **2019**, pp. 1–5.

[49] M. Wiesenfarth, M. Steiner, H. Helmers, A. W. Bett, *Sol. Energy Mater. Sol. Cells* **2021**, *219*, 110791.

[50] P. Albert, A. Jaouad, G. Hamon, M. Volatier, C. E. Valdivia, Y. Deshayes, K. Hinzer, L. Béchou, V. Aimez, M. Darnon, *Prog. Photovoltaics Res. Appl.* **2021**, *29*, 990.

[51] R. Barnett, in *Proc. - Electron. Components Technol. Conf.* **2017**, pp. 343–349.

[52] M. de Lafontaine, M. Darnon, A. Jaouad, P. Albert, B. Bouzazi, C. Colin, M. Volatier, S. Fafard, R. Arès, V. Aimez, *AIP Conf. Proc.* **2016**, *1766*, 060001.

[53] C. Domínguez, N. Jost, S. Askins, M. Victoria, I. Antón, *AIP Conf. Proc.* **2017**, *1881*, 080003.

[54] N. Jost, S. Askins, R. Dixon, M. Ackermann, C. Dominguez, I. Anton, *Sol. Energy Mater. Sol. Cells* **2022**, *240*, 111693.

[55] R. Huang, X. Q. Zhang, B. P. Ng, A. S. Kumar, K. Liu, *Int. J. Precis. Eng. Manuf. - Green Technol.* **2019**, *8*, 77.

[56] M. Roeder, T. Guenther, A. Zimmermann, *Micromachines* **2019**, *10*, 233.

[57] G. Vallerotto, I. Antón, L. S. José, R. Herrero, *Opt. Express* **2022**, *30*, 17886.

[58] L. S. José, G. Vallerotto, R. Herrero, I. Antón, *AIP Conf. Proc.* **2020**, *2298*, 050004.

[59] M. P. Lumb, K. J. Schmieder, M. González, S. Mack, M. K. Yakes, M. Meitl, S. Burroughs, C. Ebert, M. F. Bennett, D. V. Forbes, X. Sheng, *AIP Conf. Proc.* **2015**, *1679*, 040007.

[60] A. Tauke-Pedretti, J. G. Cederberg, J. L. Cruz-Campa, C. Alford, C. A. Sanchez, G. N. Nielson, M. Okandan, W. Sweatt, B. H. Jared, M. Saavedra, W. Miller, *IEEE J. Sel. Top. Quantum Electron.* **2018**, *24*, 1.

[61] J. L. Cruz-Campa, M. Okandan, P. J. Resnick, P. Clews, T. Pluym, R. K. Grubbs, V. P. Gupta, D. Zubia, G. N. Nielson, *Sol. Energy Mater. Sol. Cells* **2011**, *95*, 551.

[62] M. Ochoa, I. García, I. Lombardero, I. Rey-Stolle, C. Algora, *AIP Conf. Proc.* **2018**, *2012*, 040008.

[63] T. Nakagawa, N. Hayashi, D. Inoue, M. Matsumoto, A. Matsushita, H. Higuchi, T. Nagata, M. Ishino, K. Inoue, R. Futakuchi, M. Yamamoto, in *Optics for Solar Energy in Proc. Light, Energy and the Environment Part of Light, Energy and the Environment*, Canberra, Australia, December **2014**, p. RF4B.5.

[64] J. E. Moore, M. P. Lumb, K. J. Schmieder, R. J. Walters, B. Fisher, M. Meitl, S. Burroughs, in *2017 IEEE 44th Photovoltaic Specialist Conf. (PVSC)*, IEEE, Piscataway, NJ **2017**.

[65] W. P. Mulligan, A. Terao, S. G. Daroczi, O. C. Pujol, M. J. Cudzinovic, P. J. Verlinden, R. M. Swanson, P. Benitez, J. C. Minano, in *Conf. Record of the Twenty-Eighth IEEE Photovoltaic Specialists Conf. - 2000 (Cat. No.0°CH37036)*, IEEE, Piscataway, NJ **2000**, pp. 1495–1497.

[66] E. L. Hsiang, Z. He, Y. Huang, F. Gou, Y. F. Lan, S. T. Wu, *Crystals* **2020**, *10*, 1.

[67] D. Hwang, A. Mughal, C. D. Pynn, S. Nakamura, S. P. DenBaars, *Appl. Phys. Express* **2017**, *10*, 032101.

ADVANCED
SCIENCE NEWS

www.advancedsciencenews.com

Solar
RRL

www.solar-rrl.com

[68] I. Lombardero, M. Ochoa, N. Miyashita, Y. Okada, C. Algora, *Prog. Photovoltaics Res. Appl.* **2020**, *28*, 1097.

[69] O. Fidaner, F. A. Suarez, M. Wiemer, V. A. Sabnis, T. Asano, A. Itou, D. Inoue, N. Hayashi, H. Arase, A. Matsushita, T. Nakagawa, *Appl. Phys. Lett.* **2014**, *104*, 103902.

[70] O. Richard, A. Jaouad, B. Bouzazi, R. Arès, S. Fafard, V. Aimez, *Sol. Energy Mater. Sol. Cells* **2016**, *144*, 173.

[71] N. Hayashi, M. Terauchi, Y. Aya, S. Kanayama, H. Nishitani, T. Nakagawa, M. Takase, *AIP Conf. Proc.* **2017**, *1881*, 080005.

[72] S. Sadewasser, P. M. P. Salom, H. Rodriguez-Alvarez, *Sol. Energy Mater. Sol. Cells* **2017**, *159*, 496.

[73] M. Alves, A. Pérez-Rodríguez, P. J. Dale, C. Domínguez, S. Sadewasser, *J. Phys.: Energy* **2019**, *2*, 012001.

[74] S. Jutteau, J.-F. Guillemoles, M. Paire, *Appl. Opt.* **2016**, *55*, 6656.

[75] K. Ding, V. Avrutin, N. Izyumskaya, Ü. Özgür, H. Morkoç, *Appl. Sci.* **2019**, *9*, 1206.

[76] J. Fang, S. Liang, K. Wang, X. Xiong, K. F. Böhringer, in *2nd Annual Conf. Foundations of Nanoscience, Self-Assembled Architectures and Devices (FNANO)*, Snowbird, UT **2005**.

[77] M. Kaltwasser, U. Schmidt, L. Lösing, S. Biswas, T. Stauden, A. Bund, H. O. Jacobs, *Sci. Rep.* **2019**, *9*, 1.

[78] S. C. Park, J. Fang, S. Biswas, M. Mozafari, T. Stauden, H. O. Jacobs, *J. Microelectromech. Syst.* **2015**, *24*, 1928.

[79] S. Cho, W. Choi, S. Han, J. Kim, A. C. Lee, S. D. Kim, S. W. Song, C. Kim, D. Lee, S. Kwon, *Adv. Mater. Technol.* **2021**, *6*, 2100312.

[80] P. Y. Maeda, J. P. Lu, G. L. Whiting, D. K. Biegelsen, S. Raychaudhuri, R. Lujan, J. Veres, E. M. Chow, V. Gupta, G. N. Nielson, S. Paap, in *2015 IEEE 42nd Photovoltaic Specialist Conf., PVSC 2015*, IEEE, Piscataway, NJ **2015**, pp. 1–6.

[81] B. B. Rupp, A. Plochowietz, L. S. Crawford, M. Shreve, S. Raychaudhuri, S. Butylkov, Y. Wang, P. Mei, Q. Wang, J. Kalb, Y. Wang, *Proc. - Electron. Components Technol. Conf.* **2019**, *2019*, 1312.

[82] G. Kittler, *Eur. Solid-State Device Res. Conf.* **2019**, *2019*, 47.

[83] S. Cho, N. Kim, K. Song, J. Lee, *Langmuir* **2016**, *32*, 7951.

[84] M. P. Lumb, K. J. Schmieder, T. C. Mood, D. Baldwin, W. Wagner, J. E. Moore, M. Meitl, L. B. Ruppalt, N. A. Kotulak, J. A. Nolde, E. Armour, *Proc. SPIE - Int. Soc. Opt. Eng.* **2020**, *1127504*, 3.

[85] K. J. Schmieder, T. C. Mood, M. A. Meitl, B. Fisher, J. Carter, M. F. Bennett, E. A. Armour, M. Diaz, N. A. Kotulak, L. Ruppalt, Z. Pulwin, in *Conf. Record of the IEEE Photovoltaic Specialists Conf.*, IEEE, Piscataway, NJ **2019**, pp. 277–280.

[86] S. Y. Yang, A. Carlson, H. Cheng, Q. Yu, N. Ahmed, J. Wu, S. Kim, M. Sitti, P. M. Ferreira, Y. Huang, J. A. Rogers, *Adv. Mater.* **2012**, *24*, 2117.

[87] D. Li, T. Gu, J. Michel, J. Hu, in *Conf. Record of the IEEE Photovoltaic Specialists Conf.*, IEEE, Piscataway, NJ **2019**, pp. 2524–2527.

[88] D. Li, J. Hu, J. Michel, T. Gu, *Opt. Lett.* **2019**, *44*, 3274.

[89] P. Delaporte, A. P. Alloncle, *Opt. Laser Technol.* **2016**, *78*, 33.

[90] T. Ayari, S. Sundaram, X. Li, S. Alam, C. Bishop, W. El Huni, M. B. Jordan, Y. Halfaya, S. Gautier, P. L. Voss, J. P. Salvestrini, *ACS Photonics* **2018**, *5*, 3003.

[91] R. Mertens, **2019**, https://www.microled-info.com/digitimes-eosrl-achieved-breakthrough-its-micro-led-transfer-process (accessed: July 2020).

[92] V. W. Lee, N. Twu, I. Kymissis, *Inf. Disp.* **2016**, *32*, 16.

[93] J. E. Moore, K. J. Schmieder, W. Wagner, M. P. Lumb, *J. Photonics Energy* **2019**, *9*, 014501.

[94] A. Rudorfer, M. Tscherner, C. Palfinger, F. Reil, P. Hartmann, I. E. Seferis, E. Zych, F. P. Wenzl, *Fifteenth Int. Conf. Solid State Light. LED-Based Illum. Syst.* **2016**, *9954*, 99540E.

[95] Q. Huang, Y. Zhu, *Adv. Mater. Technol.* **2019**, *4*, 1.

[96] J. Suikkola, T. Björninen, M. Mosallaei, T. Kankkunen, P. Iso-Ketola, L. Ukkonen, J. Vanhala, M. Mäntysalo, *Sci. Rep.* **2016**, *6*, 25784.

[97] W. J. Hyun, S. Lim, B. Y. Ahn, J. A. Lewis, C. D. Frisbie, L. F. Francis, *ACS Appl. Mater. Interfaces* **2015**, *7*, 12619.

[98] Y. Hong, B. Lee, J. Byun, E. Oh, H. Kim, S. Kim, S. Lee, D. Kim, J. Yoon, *Dig. Tech. Pap. - SID Int. Symp.* **2017**, *48*, 253.

[99] R. S. Cok, M. Meitl, R. Rotzoll, G. Melnik, A. Fecioru, A. J. Trindade, B. Raymond, S. Bonafede, D. Gomez, T. Moore, C. Prevatte, *J. Soc. Inf. Disp.* **2017**, *25*, 589.

[100] H. Zheng, L. Li, X. Lei, X. Yu, S. Liu, X. Luo, *IEEE Electron Device Lett.* **2014**, *35*, 1046.

[101] C. A. Bower, *Micro-Transfer-Printing (µTP): Technology Overview*, Institute of Electrical and Electronics Engineers **2014**, https://site.ieee.org/ocs-cpmt/files/2013/06/CPMT_2014.02.11_V1_uTP.pdf (accessed: June 2020).

[102] B. J. Kim, C. Lee, Y. Jung, K. Hyeon Baik, M. A. Mastro, J. K. Hite, C. R. Eddy, J. Kim, *Appl. Phys. Lett.* **2011**, *99*, 143101.

[103] L. Barrutia, I. Lombardero, M. Ochoa, M. Gabas, I. Garcia, T. Palacios, A. Johnson, I. Rey-Stolle, C. Algora, *Prog. Photovoltaics Res. Appl.* **2020**, *28*, 60.

[104] X. Guo, C. W. Guo, C. Wang, C. Li, X. M. Sun, *Nanoscale Res. Lett.* **2014**, *9*, 670.

[105] K. Ghosal, B. Fisher, D. Lilly, J. Gabriel, S. Seel, S. Burroughs, *IEEE J. Photovoltaics* **2016**, *6*, 1360.

[106] N. Yamada, D. Hirai, *Prog. Photovoltaics Res. Appl.* **2016**, *24*, 846.

[107] G. N. Nielson, M. Okandan, J. L. Cruz-Campa, A. L. Lentine, W. C. Sweatt, B. H. Jared, P. J. Resnick, B. Kim, B. J. Anderson, V. P. Gupta, A. Tauke-Pedretti, in *Conf. Record of the IEEE Photovoltaic. Specialists Conf.*, IEEE, Piscataway, NJ **2013**, pp. 465–469.

[108] T. Gu, W. C. Sweatt, G. Agrawal, B. H. Jared, B. J. Anderson, R. S. Goeke, B. Elisberg, S. M. Paap, J. L. Cruz-Campa, V. Gupta, M. Okandan, *SPIE Opt. Eng. Appl.* **2014**, *9191*, 91910G.

[109] D. Li, L. Li, B. Jared, G. Keeler, B. Miller, M. Wood, C. Hains, W. Sweatt, S. Paap, M. Saavedra, C. Alford, *Prog. Photovoltaics Res. Appl.* **2018**, *26*, 651.

[110] T. Gu, J. Hu, US20170352771A1, **2017**.

[111] N. Yamada, T. Ijiro, W. Goto, K. Okamoto, K. Dobashi, T. Shiobara, in *Conf. Record of the IEEE Photovoltaic Specialists. Conf.*, IEEE, Piscataway, NJ **2013**, pp. 493–496.

[112] N. Jost, C. Dominguez, G. Vallerotto, T. Gu, J. Hu, I. Anton, in *Conf. Record of the IEEE Photovoltaic Specialists Conf.*, Chicago, IEEE, Piscataway, NJ **2019**, pp. 249–254.

[113] J. Gong, G. Violakis, D. Infante, P. Hoffmann, A. Kostro, A. Schüler, in *Laser-based Micro- and Nanoprocessing XII*, San Francisco, CA, January–February **2018**, p. 37.

[114] A. Terao, W. P. Mulligan, S. G. Daroczi, O. C. Pujol, P. J. Verlinden, R. M. Swanson, J. C. Minano, P. Benitz, J. L. Alvarez, in *Conf. Record of the IEEE Photovoltaic Specialists Conf.*, vol. *2000*, IEEE, Piscataway, NJ January 2000, pp. 1416–1419.

[115] P. Voarino, A. Ritou, C. Seraine, M. Roux, R. Couderc, *AIP Conf. Proc.* **2019**, *2149*, 050008.

[116] R. M. Beal, M. Wilkins, J. F. Wheeldon, J. E. Haysom, C. E. Valdivia, M. Yandt, P. Dufour, S. Myrskog, J. Fan, H. Navarro, J. P. Morgan, *AIP Conf. Proc.* **2011**, *1407*, 239.

[117] J. H. Karp, J. E. Ford, *SPIE Sol. Energy+ Technol.* **2009**, *7407*, 74070D.

[118] C. Leiner, C. Sommer, V. Satzinger, L. Plessing, G. Peharz, *AIP Conf. Proc.* **2016**, *1766*, 080002.

[119] S. Cui, N. P. Lyons, L. R. Diaz, R. Ketchum, K. J. Kim, H. C. Yuan, M. Frasier, W. Pan, R. A. Norwood, *Opt. Express* **2019**, *27*, A572.

[120] S. Bouchard, S. Thibault, *Opt. Express* **2014**, *22*, A248.

[121] M. Nam, K. Kim, J. Lee, K. K. Lee, S. S. Yang, *Sol. Energy* **2013**, *91*, 374.

[122] C. J. Ruud, A. J. Grede, J. K. Chang, M. P. Lumb, K. J. Schmieder, B. Fisher, J. A. Rogers, J. M. Gordon, N. C. Giebink, *Opt. Express* **2019**, *27*, A1467.

[123] C. J. Ruud, J. M. Gordon, R. McCarthy, B. Fisher, N. C. Giebink, in *Conf. Record of the IEEE Photovoltaic. Specialists Conf.*, IEEE, Piscataway, NJ **2021**, pp. 1289–1292.

[124] G. Sala, E. Lorenzo, *J. Appl. Metalwork.* **1979**, *1*, 1004.

[125] N. Jost, G. Vallerotto, C. Domínguez, S. Askins, I. Antón, *AIP Conf. Proc.* **2019**, *2149*, 070006.

[126] N. Jost, G. Vallerotto, A. Tripoli, S. Askins, C. Domínguez, I. Antón, *Sol. Energy Mater. Sol. Cells* **2022**, *245*, 111882.

[127] N. Jost, G. Vallerotto, A. Tripoli, B. D. L'Eprevier, C. Domínguez, S. Askins, I. Antón, *AIP Conf. Proc.* **2020**, *2298*, 050003.

[128] A. Jacobo-Martín, N. Jost, J. J. Hernández, C. Domínguez, G. Vallerotto, S. Askins, I. Antón, I. Rodríguez, *Opt. Express* **2021**, *29*, 34135.

[129] M. Z. Shvarts, V. M. Emelyanov, M. V. Nakhimovich, A. A. Soluyanov, V. M. Andreev, *AIP Conf. Proc.* **2019**, *2149*, 070011.

[130] N. Ikawa, S. Shimada, H. Tanaka, *Nanotechnology* **1992**, *3*, 6.

[131] N. C. R. Holme, T. W. Berg, P. G. Dinesen, *Laser Beam Shap. IX* **2008**, *7062*, 70620J.

[132] Y. Takeuchi, S. Maeda, T. Kawai, K. Sawada, *CIRP Ann.* **2002**, *51*, 343.

[133] K. Liu, B. Lauwers, D. Reynaerts, *Int. J. Adv. Manuf. Technol.* **2009**, *47*, 11.

[134] T. Mappes, M. Worgull, M. Heckele, J. Mohr, *Microsyst. Technol.* **2008**, *14*, 1721.

[135] C. G. Blough, J. P. Bowen, R. L. Michaels, *Appl. Opt.* **1997**, *36*, 8970.

[136] R. Murali, D. K. Brown, K. P. Martin, J. D. Meindl, *J. Vac. Sci. Technol., B* **2006**, *24*, 2936.

[137] S. Y. Chou, P. R. Krauss, P. J. Renstrom, *Appl. Phys. Lett.* **1998**, *67*, 3114.

[138] M. Weiser, *Nucl. Instrum. Methods Phys. Res., Sect. B* **2009**, *267*, 1390.

[139] T. Masuzawa, *CIRP Ann.* **2000**, *49*, 473.

[140] J. Yuan, B. Lyu, W. Hang, Q. Deng, *Front. Mech. Eng.* **2017**, *12*, 158.

[141] D. Sato, K. Tanino, N. Yamada, *Sol. Energy Mater. Sol. Cells* **2020**, *208*, 110396.

[142] M. Schaub, J. Schwiegerling, E. C. Fest, A. Symmons, R. H. Shepard, *J. Chem. Inf. Model.* **2013**, *53*, 1689.

[143] S. Bäumer, *Handbook of Plastic Optics*, 2nd ed., John Wiley & Sons, Inc. **2011**, ISBN: 978-3-527-63545-0.

[144] T. Luce, J. Cohen, in *Conf. Record of the IEEE Photovoltaic Specialists Conf.*, IEEE, Piscataway, NJ **2010**, pp. 487–492.

[145] C. Peixoto, P. T. Valentim, P. C. Sousa, D. Dias, C. Araújo, D. Pereira, C. F. Machado, A. J. Pontes, H. Santos, S. Cruz, *Precis. Eng.* **2022**, *76*, 29.

[146] S. H. M. Kersjes, J. L. J. Zijl, R. H. Poelma, H. W. Wensink, in *2013 European Microelectronics Packaging Conf. (EMPC 2013)*, Grenoble, France, September **2013**.

[147] Y. K. Kim, M. R. Haq, S.-M. Kim, *Opt. Express* **2019**, *27*, 1553.

[148] S. W. Kuhn, F. Pahmer, US20120282438A1, **2012**.

[149] N. Kooy, K. Mohamed, L. T. Pin, O. S. Guan, *Nanoscale Res. Lett.* **2014**, *9*, 320.

[150] N. Tucher, O. Höhn, H. Hauser, C. Müller, B. Bläsi, *Microelectron. Eng.* **2017**, *180*, 40.

[151] N. Unno, S. Kakimoto, T. Mäkelä, S. Hiwasa, J. Taniguchi, *J. Adv. Mech. Des. Syst. Manuf.* **2018**, *12*, JAMDSM0101.

[152] S. Meng, Z. Yin, Y. Guo, J. Yao, N. Chai, *Int. J. Adv. Manuf. Technol.* **2020**, *108*, 2445.

[153] I. Navarro-Baena, A. Jacobo-Martín, J. J. Hernández, J. R. C. Smirnov, F. Viela, M. A. Monclús, M. R. Osorio, J. M. Molina-Aldareguia, I. Rodríguez, *Nanoscale* **2018**, *10*, 15496.

[154] C. Steinberg, N. Al-Hussainawi, M. Papenheim, A. Mayer, H. C. Scheer, M. Matschuk, H. Pranov, *J. Vac. Sci. Technol., B* **2017**, *35*, 06G306.

[155] L. Peng, Y. Deng, P. Yi, X. Lai, *J. Micromech. Microeng.* **2014**, *24*, 013001.

[156] Y. Deng, P. Yi, L. Peng, X. Lai, Z. Lin, *J. Micromech. Microeng.* **2015**, *25*, 065004.

[157] N. Vaidya, O. Solgaard, *Microsyst. Nanoeng.* **2018**, *4*, 18.

[158] A. Zolfaghari, T. Chen, A. Y. Yi, *Int. J. Extreme Manuf.* **2019**, *1*, 012005.

[159] I. Basak, K. Paivasaari, *North. Opt. Photonics* **2015**, *2015*, 3.

[160] H. Apostoleris, M. Stefancich, M. Chiesa, *Nat. Energy* **2016**, *1*, 16018.

[161] H. J. D. Johnsen, A. Aksnes, J. Torgersen, in *Proc. Volume 11120, Nonimaging Optics: Efficient Design for Illumination and Solar Concentration XVI; 111200B*, San Diego, CA, **2019**.

[162] M. P. Lumb, K. J. Schmieder, T. C. Mood, M. F. Bennett, A. Taploo, J. E. Moore, D. Scheiman, E. Armour, B. Fisher, M. Meitl, J. Carter, in *Conf. Record of the IEEE Photovoltaic Specialists. Conf., Chicago*, IEEE, Piscataway, NJ **2019**, pp. 2528–2532.

[163] D. Sato, K. H. Lee, K. Araki, T. Masuda, M. Yamaguchi, N. Yamada, *IEEE J. Photovoltaics* **2018**, *9*, 147.

[164] J. F. Martínez, M. Steiner, M. Wiesenfarth, T. Fellmeth, T. Dörsam, M. Wiese, S. W. Glunz, F. Dimroth, *Prog. Photovoltaics Res. Appl.* **2020**, *28*, 349.

[165] D. Li, Q. Zhang, T. Gu, J. Hu, in *Conf. Record of the IEEE Photovoltaic Specialists Conf.*, IEEE, Piscataway, NJ **2019**, pp. 1624–1627.

[166] J. F. Martínez Sánchez, M. Steiner, M. Wiesenfarth, H. Helmers, G. Siefer, S. W. Glunz, F. Dimroth, *SSRN Electron. J.* **2021**, http://dx.doi.org/10.2139/ssrn.3815001.

[167] M. Wiesenfarth, D. Iankov, J. F. Martínez, P. Nitz, M. Steiner, F. Dimroth, H. Helmers, *AIP Conf. Proc.* **2022**, *2550*, 030008.

[168] M. Xiao, L. Tang, X. Zhang, I. Y. F. Lun, Y. Yuan, *Energies* **2018**, *11*, 3416.

[169] N. Hayashi, D. Inoue, M. Matsumoto, A. Matsushita, H. Higuchi, Y. Aya, T. Nakagawa, *Opt. Express* **2015**, *23*, A594.

[170] A. Ritou, P. Voarino, S. Bernardis, T. Hilt, A. Aitmani, C. Dominguez, M. Baudrit, *AIP Conf. Proc.* **2016**, *1766*, 080005.

[171] A. Ritou, P. Voarino, O. Raccurt, *Sol. Energy* **2018**, *173*, 789.

[172] O. Kückmann, *Light. Diodes Res. Manuf. Appl. X* **2006**, *6134*, 613404.

[173] E. Chinello, M. A. Modestino, L. Coulot, M. Ackermann, F. Gerlich, D. Psaltis, C. Moser, *Global Challenges* **2017**, *1*, 1700095.

[174] M. Sinclair, P. Dufour, K. Drew, S. Myrskog, J. P. Morgan, *High Low Conc. Syst. Sol. Energy Appl. IX* **2014**, *9175*, 91750P.

[175] A. Ritou, P. Voarino, B. Goubault, N. David, S. Bernardis, O. Raccurt, M. Baudrit, *AIP Conf. Proc.* **2017**, *1881*, 030007.

[176] G. Nardin, A. F. Aguilar, L. Anglade, M. Duchemin, F. Gerlich, M. Ackermann, L. Coulot, D. Petri, J. Levrat, A. Faes, J. Champliaud, *AIP Conf. Proc.* **2019**, *2149*, 040001.

[177] D. Sato, K. H. Lee, K. Araki, M. Yamaguchi, N. Yamada, *IEEE J. Photovoltaics* **2019**, *9*, 147.

[178] J. F. Martinez, M. Steiner, M. Wiesenfarth, G. Siefer, S. W. Glunz, F. Dimroth, in *Conf. Record of the IEEE Photovoltaic Specialists Conf.*, Vol. *2020*, IEEE, Piscataway, NJ **2020**, pp. 2708–2711.

[179] U. Srinivasan, D. Liepmann, R. T. Howe, *J. Microelectromech. Syst.* **2001**, *10*, 17.

[180] R. Fischbach, T. Horst, J. Lienig, in *IEEE 2019 Int. 3D Systems Integration Conf. 3DIC 2019*, IEEE, Piscataway, NJ **2019**.

[181] V. R. Marinov, *SID Symp. Dig. Tech. Pap.* **2018**, *49*, 692.

[182] A. C. Fischer, J. G. Korvink, N. Roxhed, G. Stemme, U. Wallrabe, F. Niklaus, *J. Micromech. Microeng.* **2013**, *23*, 083001.

[183] K. Baker, J. Karp, J. Hallas, J. Ford, *Nonimaging Opt. Effic. Des. Illum. Sol. Conc. IX* **2012**, *8485*, 848504.

[184] X. Liu, Z. Lu, R. Leto, C. Brule, N. Brates, in *2017 IEEE 44th Photovoltaic Specialist Conf. (PVSC)*, IEEE, Piscataway, NJ **2017**, pp. 1728–1732.

[185] R. Leto, N. Brates, C. Brule, Z. J. Lu, X. Liu, in *2018 IEEE 7th World Conf. Photovoltaic Energy Conversion, WCPEC 2018 - A Jt. Conf. 45th IEEE PVSC, 28th PVSEC 34th EU PVSEC*, IEEE, Piscataway, NJ **2018**, pp. 2697–2702.

[186] V. Zagolla, D. Dominé, E. Tremblay, C. Moser, *Opt. Express* **2014**, *22*, A1880.

Norman Jost is a researcher in photovoltaic solar energy. He received his B.Eng. degree in photovoltaic and semiconductor technology from the Ernst-Abbe Hochschule in Jena and his M.S. degree in the same field from the TU Bergakademie Freiberg in Germany. In 2022, he attained his Ph.D. degree from the Universidad Politecnica of Madrid in the field of photovoltaic solar energy. His research interests include high-efficiency solar cells for space applications and concentrator photovoltaics, characterization of multijunction solar cells, optics for concentration, power modeling, and design of photovoltaic solar energy plants.
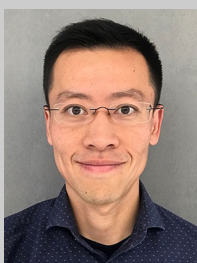
Tian Gu is a research scientist and principal investigator at the Materials Research Laboratory and Department of Materials Science and Engineering at MIT. His research interests involve metasurface optics, integrated photonics, and photonic materials. Dr. Gu is a recipient of the SPIE Rising Researcher Award, R&D 100 Award, TechConnect National Innovation Award, among others. He has served on the conference program committees for CPV-X, CLEO, IEEE Summer Topicals Meeting, IEEE Photonics Conference, Optical Interconnects Conference, SENSORS, International Congress on Glass, etc. He also serves on the Editorial Board of Scientific Reports.

Juejun (JJ) Hu is currently the John F. Elliott Professor of Materials Science and Engineering at MIT. His research primarily focuses on integrated photonics and metasurface optics. Prof. Hu has authored and coauthored more than 150 refereed journal publications, and he has been recognized with the SPIE Early Career Achievement Award, the Robert L. Coble Award from the American Ceramic Society, the Vittorio Gottardi Prize from the International Commission on Glass, the NSF CAREER award, and the DARPA Young Faculty Award, among others. Hu is a fellow of Optica, SPIE, and the American Ceramic Society.

César Domínguez received his M.Sc. degree in telecommunications engineering in 2004 and his Ph.D. degree in photovoltaic solar energy in 2012 (Prof. Gabriel Sala's group), both from Universidad Politécnica de Madrid. His Ph.D. thesis at the Solar Energy Institute demonstrated the first commercial solar simulator for concentrator PV modules, installed worldwide. He worked as a research engineer at CEA-INES and carried out research stays at Fraunhofer ISE and MIT. He leads a research line on micro-concentrators applied to high-efficiency, building-integrated, and space-based PV modules. He is an associate professor at ETS Ingeniería y Diseño Industrial since 2015.

Ignacio Antón received his M.S. degree in telecommunication engineering from the Universidad Politécnica de Madrid (UPM) in 1998 and his Ph.D. degree from the Instituto de Energía Solar (IES), belonging to the UPM, in 1998 on the topic of methods and equipment for the characterization of concentrating photovoltaic systems. He is full professor at UPM and head of the Instruments and Systems Integration research group at IES. He has published more than 200 papers in scientific journals and international conferences, participated in the scientific committee of several international PV conferences and is member of the IEC TC82 focused on the development of international standards related to CPV and VIPV.